LA-6018-PR

Progress Report

Applied Nuclear Data

Research and Development

January 1—March 31, 1975

Compiled by

P. G. Young

los alamos
scientific laboratory
of the University of California
LOS ALAMOS, NEW MEXICO 87545

An Affirmative Action/Equal Opportunity Employer

The four most recent reports in this series, unclassified, are:

In the interest of prompt distribution, this report was not edited by the
Technical Information staff.

CONTENTS

APPLIED NUCLEAR DATA RESEARCH AND DEVELOPMENT

QUARTERLY PROGRESS REPORT

January 1 through March 31, 1975

Compiled by

P. G. Young

ABSTRACT

This progress report describes the activities of the Los Alamos Nuclear
Data Group for the period January 1 through March 31, 1975. The topical con-
tent of this report is summarized in the Contents.

I. THEORY AND EVALUATION OF NUCLEAR CROSS SECTIONS

A. R-Matrix Analysis of Light Element Standards (G. M. Hale)

Cross sections for the (n,α) reactions on ^{10}B
and ^6Li are useful standards at low energies ($E_n <$
50 keV) since they follow the $1/v$ energy dependence.
Because these cross sections are also used as stand-
ards at higher energies where resonance structure is
evident, we have been performing comprehensive R-
matrix analyses of reactions in the ^{11}B and ^7Li sys-
tems with the goal of providing accurate (n,α) cross
sections in the region $0 \leqslant E_n \leqslant 1$ MeV.

It has been found that data from the charged-
particle reactions provide critical information in
these analyses. For the ^{11}B system, most of the
resonances in the region of interest are strongly
evident in the $\alpha + {}^7Li$ reactions, so that these re-
actions are being used to identify resonances which
affect the $^{10}B(n,\alpha)$ cross sections. In the ^7Li sys-
tem, recent precision measurements of $\alpha + t$ elastic
differential cross section[1] have been used in con-
junction with other data to obtain an indirect but
stringent determination of the $^6Li(n,\alpha)$ cross sec-
tion in the region of the 240-keV resonance.

An interesting test of the ^7Li analysis was
provided by new preliminary measurements of the
$^6Li(\vec{n},\alpha)$ analyzing power[2] which indicate unexpected-
ly large neutron polarizations (~90%) near 1 MeV.
The analysis indeed predicts neutron analyzing pow-

ers in excess of 90% at energies near 1 MeV. This
new feature makes ^6Li possibly of interest as a neu-
tron polarimeter.

B. GNASH – A Multipurpose Statistical Theory Code (P. G. Young and E. D. Arthur)

A multipurpose statistical theory code (GNASH)
has been developed for calculating neutron, gamma-
ray, and charged-particle energy spectra from almost
any combination of neutron-induced reactions at neu-
tron energies up to 20 MeV or higher. In addition
to spectra, the code permits calculation of level
excitation and gamma-ray de-excitation cross sections
for up to 50 discrete levels in any residual nuclei
involved in a problem, thus permitting determination
of activation cross sections and isomer ratios.

Widths for particle decay are computed from op-
tical model transmission coefficients, and gamma-ray
widths are presently calculated using either the
Weisskopf single-particle approximation or a giant
dipole resonance model. Gamma-ray emission by elec-
tric and magnetic dipole or quadrupole transitions
are permitted, and gamma-ray cascades are followed
in detail. A pre-equilibrium model is used to ac-
count for semi-direct processes. The Gilbert and
Cameron[3] form of level density function is presently
used and is matched with inputted discrete data for
low-lying states in each residual nucleus. The code
is structured such that improved representations of
level densities, gamma-ray widths, and pre-equilib-
rium processes can be easily incorporated.

Preliminary calculations[4] have been performed for neutron-induced reactions on ^{181}Ta with thermal neutrons and on ^{93}Nb with 14-MeV neutrons, and comparisons have been made with experimental gamma-ray spectra. Figure 1 shows the 14-MeV ^{93}Nb$(n,x\gamma)$ spectrum measurement by Drake et al.[5] (crosses) and the ENDF/B-IV evaluation (solid curve). The dashed curve shows the GNASH calculation using a giant dipole resonance model to compute gamma-ray widths, and the dash-dot curve shows a similar calculation using the Weisskopf approximation. In both cases, neutron transmission coefficients computed from global optical model parameters[6] were used, and no attempt was made to optimize them. A value of $a = 14$ MeV^{-1} was used for the level density parameter.

The giant dipole resonance approximation results in better overall agreement with the experiment for reasonable level density parameters. The calculated total (n,2n) cross section and the (n,2n) cross section to the isomeric first excited state of ^{92}Nb both agree with experiment to about 20%.

Detailed analyses of the available experimental data for several nuclear systems are planned for the near future.

C. Re-evaluation of the n + ^{6}Li Data File (L. Stewart, P. G. Young, and V. Stovall)

This effort is limited to neutron energies above 500 keV. A preliminary survey indicates that all energy-dependent cross sections will be changed from the ENDF/B-IV file with the possible exception of the (n,t) reaction. Since time does not permit a complete "in-depth" study, only recent measurements are being compared with the old evaluation to determine whether changes should be incorporated.

An important part of this effort will be directed toward provision of consistent energy-angular distributions for the (n,n'd) and (n,2n) neutrons; the new distributions will conserve energy in the reactions.

The difficulty in conserving cross section remains; that is, measurements of the partial cross sections rarely sum to agree with experiments on σ_{tot} in this energy range. At a few energies, these disagreements are quite large. An effort is underway to try to determine upper and lower limits on these energy assignments.
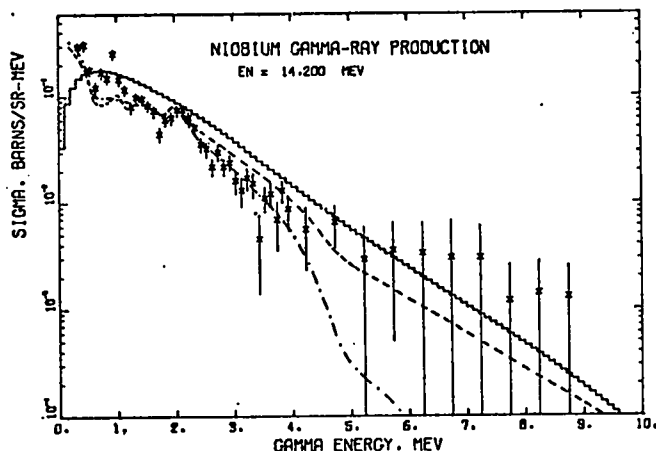
Fig. 1. Measured and calculated gamma-ray spectra from bombardment of ^{93}Nb with 14-MeV neutrons.

D. Evaluation of Neutron-Induced Reactions on ^{15}N (E. D. Arthur, G. M. Hale, and P. G. Young)

The neutron-induced reactions on ^{15}N other than scattering generally have high-lying thresholds ($E_n \sim 8$ MeV). The enrichment of nitride-based reactor fuels with ^{15}N therefore offers the possibility of reducing the undesirable neutron absorption and helium production that occur for ^{14}N-based fuels, particularly in fast reactors.[7]

We are evaluating cross sections for all the neutron-induced reactions on ^{15}N below 20 MeV. At energies below about 6 MeV, the evaluation is based on an R-matrix analysis which will represent the detailed structure of the cross sections. The R-matrix analysis in progress was started from the level scheme reported by Zeitnitz et al.[8] Our preliminary fit indicates some changes in that level scheme may be required.

At energies above ~6 MeV, the few cross sections that have been measured show little resolved resonance structure. The evaluation between about 6 and 20 MeV therefore will be based upon calculations performed with our general-purpose statistical-model code, GNASH. We have begun to generate the optical model transmission coefficients required for these calculations by adjusting the global parameters of Wilmore and Hodgson[6] to obtain good fits to the ^{15}N neutron total cross section in the range from 10 to 20 MeV.

E. Time-Dependent Gamma-Ray Spectra from Fission of ^{235}U and ^{239}Pu (D. G. Foster, Jr.)

An evaluation has been completed of the spectrum and intensity of gamma rays following neutron-induced fission of ^{235}U and ^{239}Pu, covering the time interval from the prompt burst to 60 s. Since the immediate need was to provide data between 1 μs and the plateau region for a particular application, the evaluation is based on only the most recent measurements, and no attempt has been made to reconcile conflicting measurements or to cover regions devoid of measurements by any kind of theoretical considerations. In particular, changes in yield or spectrum as a function of the energy of the incident neutron have been ignored. The results of the evaluation are available in the recently established ENDF/B format.

The data considered for this evaluation were taken from a series of papers by Sund and collaborators[9-12] for times up to the plateau in the ms region, and from Fisher and Engle[13] for times from the ms range to 1 min. The prompt (<1 ns) spectrum and intensity were read from the published graphs[9] and binned in 33 groups. The data from the low ns range to 1 μs are available as resolved lines plus an unresolved continuum taken from a Ge(Li) measurement.[9] Since the continuum is given as integrals over five time intervals between 20 and 958 ns, these data were fitted assuming two simple exponentially decaying components in each of five energy bins. The resulting parameterization was used to calculate yield histograms over the entire time range from 1 ns to 60 s, using 7 steps per decade in time. A simple smoothing algorithm was then applied to split each histogram into bins, which were then rebinned into 14 groups with more convenient boundaries.

In the μs range, NaI measurements[11,12] have revealed six strong lines with no significant continuous background. These lines were included with the resolved lines from the Ge(Li) measurements at earlier times and the continuum from earlier times simply extrapolated into the μs region. The complete set of lines was examined for known cascades. The half-life of each cascade was averaged from the observed half-lives of the component lines, using both ^{235}U and ^{239}Pu data if the lines were observed in both isotopes. Where the yields of the individ-

ual lines were equal within experimental error, it was assumed that the decay is sequential, so the yields were also averaged.

The data of Fisher and Engle[13] were published in their fully corrected form, as 17-group gamma-ray histograms averaged over 5 time intervals between 0.2 and 45 s. These were treated in essentially the same way as the unresolved continuum in the ns range; namely, by fitting the integrals as a function of time with two simple exponentials in order to interpolate and extrapolate. The 17-bin histograms as a function of time calculated from these parameters were then converted to the same bin structure as used for the early-time continuum. The time scale was cut off at 60 s, which represents a modest extrapolation from the Fisher-Engle data and permits a reasonable overlap with calculations which can be done using detailed knowledge of the yields and decay schemes of individual fission products with the help of codes such as CINDER.

The ENDF/B representation of the evaluation uses both File 17 (resolved lines) and File 18 (continuum vs time). The overall intensity is dominated by the prompt burst in File 18 below 1 ns, by the resolved lines from there to a few hundred μs, and then by the continuum for the rest of the time range covered by the evaluation. The continuum is represented by 34 groups in the prompt spectrum, 15 groups from there to 1 μs, and 16 groups thereafter, in order to represent the available data as compactly as possible.

The completed evaluation reveals that the overall multiplicity integrated up to 60 s after fission is 11.9 photons/fission for ^{235}U and 12.4 photons/fission for ^{239}Pu. The average energy of the photons is 0.92 MeV in the prompt burst, drops to 0.40 MeV at 1 ns, and rises gradually to about 1.0 MeV at 60 s.

The overall accuracy of both the intensity and the spectrum is estimated to be about 20% at all times. It seems likely that between 1 μs and a few ms the intensity of the continuum is low by up to 10%. Since no photons above 1.4 MeV are given in any of the recent data between 1 ns and 1 ms, it is likely that the average energy of the photons is low over this entire range of times.

II. NUCLEAR CROSS SECTION PROCESSING

Group T-2 is supporting and developing a variety of computer codes for processing evaluated nuclear data into forms that can be used for design purposes. It is also producing processed data sets for various national and Los Alamos Scientific Laboratory (LASL) programs. The following subsections summarize recent progress.

A. Cross Section Production (R. B. Kidman, R. E. MacFarlane, D. W. Muir, and R. J. Barrett)

The 50-group 22-isotope and 240-group 5-isotope libraries produced last quarter plus the CCCC utility codes LINX, BINX, and CINX were written on magnetic tapes and sent to Hanford Engineering Development Laboratory (HEDL), Brookhaven National Laboratory (BNL), Argonne National Laboratory (ANL), General Atomic (GA), General Electric (GE), and Westinghouse Advanced Reactor Division (WARD). The purpose of this release was to exercise systems using the CCCC-III interface[14] and to obtain feedback on the MINX data and utility codes. The data were also to be used for the Cross Section Evaluation Working Group (CSEWG) phase II data testing of the Evaluated Nuclear Data File B-IV (ENDF/B-IV).

Several laboratories have converted LINX, BINX, and CINX to IBM machines. In addition to the normal problems of machine incompatibility, several errors were discovered in the group collapse code CINX: the principal cross sections on the ISOTXS file were being written twice, the LOCA array was incorrect, a pointer word was being computed incorrectly which caused an error in the principal cross sections, and the inelastic cross section array was not being correctly initialized. These errors have been corrected.

Reported errors in the cross section data are as follows: the ^{238}U inelastic is incorrect, the fission χ vector is in backwards, and the thermal group is incorrectly weighted. The first error is apparently due to running MINX in a 240-group structure and does not occur for 50-group runs. The other two errors have been corrected.

Cross sections have been generated in the LASL 30-group structure for ^{235}U, ^{238}U, and ^{239}Pu from ENDF/B-IV incorporating the effects of the partial fission reactions[15] for the LASL Theoretical Design Division. Cross sections have also been generated for use in the LASL CTR neutronics program.

The latest version of ENDF/B-IV has been obtained from the National Neutron Cross Section Center (NNCSC) and BNL. These files are available to LASL users on photostore.

Work on cross sections for the Nuclear Reactor Safety Test Facility has continued in cooperation with LASL group T-DOT. A modified version of 1DX[16] was obtained from HEDL and made operational on the CDC 7600. This version provides more accurate heterogeneity corrections for a variety of fuel geometries.

B. MINX Code Development (R. B. Kidman, R. E. MacFarlane, D. W. Muir, R. M. Boicourt)

The way MINX handles the potential scattering cross section for the CCCC BRKOXS file has been extensively modified. Pointwise potential scattering cross sections are now saved on the PENDF tape so that MINX restart runs from PENDF tapes will provide potential scattering cross sections for the BRKOXS file. Also, the computation of the BRKOXS potential scattering cross sections has been changed from the previous constant value of $4\pi a^2$ to the energy dependent form used in the resonance range. The values given at higher energies may not be meaningful.

The inelastic cross sections for the CCCC BRKOXS file have been modified to be the sum of the (n,n') and (n,3n) reactions. Previously, three times the (n,3n) reaction has been added. This modification allows the total reaction cross sections to balance with the sum of their constituent reactions.

The fission χ vector (in the CCCC ISOTXS file) was found to be in inverse order. MINX was modified to write the vector in the correct order.

One of the MINX flux weighting options is a linking of three spectra -- thermal, 1/E, and fission. The form of the thermal spectrum was incorrectly given as the Maxwellian spectrum rather than a Maxwellian flux. This error has been corrected. The nuclear temperatures and the breakpoint energies between the region can be specified by the user so as to give group cross sections appropriate to any particular application.

The computer code CINX has been completed. CINX can be used to collapse cross sections on CCCC-III, ISOTXS, and BRKOXS files to a subset group structure using fine-group fluxes specified by the user. If the user's flux is the same as the flux used to generate the original fine-group library, the collapse

will be exact in the sense that the resulting coarse-group cross sections will be the same as those obtained by running MINX from scratch.

CINX can also be used to combine the cross sections on ISOTXS and BRKOXS files into the format required by 1DX.[16] This option makes the MINX cross sections readily available to a great number of reactor physics codes.

C. Processing Code Validation (R. E. MacFarlane, R. B. Kidman, D. W. Muir, and R. J. Barrett)

The Processing Code Subcommittee of the Code Evaluation Working Group held its first meeting in Washington, D.C., on March 2, 1975, sponsored by the Energy Research and Development Administration's Reactor Research and Development Branch (ERDA/RRD). It was chaired by R. E. MacFarlane and attended by representatives from ERDA, ANL, Holifield National Laboratory (HNL), WARD, GE, BNL, and HEDL. The purpose of this meeting was to outline a program of tests and comparisons designed to validate the various cross section processing codes needed for the design and analysis of fast reactor cores and critical assemblies.

The participants chose an infinite homogeneous system for initial studies. Both integral and differential properties will be compared. Sensitivity methods will be used to find the sources of the most important differences between the codes. The differences found will be analyzed, and attempts to resolve them will be made.

Beginning next fiscal year, the participants will analyze a general finite inhomogeneous problem based on the unspiked ZPPR inner core cell.[17] Integral results from various codes will be compared with each other and with "exact" Monte Carlo calculations. Sensitivity analysis will be used to locate important sources of differences.

In all of the comparison work, an attempt will be made to separate errors from inherent differences due to choices of algorithms. Effects of options, advantages, and disadvantages of various codes, and suggestions for future work will also be reported.

Preparations for LASL participation in this program and in the CSEWG data testing program have continued this quarter. They include bringing various codes to operational status and generating cross sections for the isotopes needed.

D. Self-Shielding of Elastic Group-to-Group Transfer Cross Sections (R. E. MacFarlane and M. Becker [RPI])

The self-shielding factor method[18,19] for preparing group constants has been adopted widely, particularly for fast reactor analysis. In most applications of this method to date,[16,20-22] the elastic scattering effects have been represented by an elastic removal or downscatter cross section, σ_d. Although gross spectral shape is accounted for by iterating a group-wise flux calculation, resonance self-shielding effects on the elastic removal cross section are assumed to be the same as those for the elastic cross section.

In the new MINX/SPHINX code system, these approximate representations of elastic scattering effects are replaced by an actual numerical evaluation of the elastic transfer matrix elements including a full treatment of anisotropy. One advantage of this approach is that the location of a resonance within the group is accounted for properly. The absence of such accounting has been cited[23] as a shortcoming of the shielding factor codes. In addition, the accurate representation of scattering to more than one group makes the use of finer group structures possible. This in turn allows for more accurate treatment of gross flux variations such as those caused by the important sodium and iron resonances.

However, the development of the MINX/SPHINX system has been limited to date by the same assumption used in the earlier codes; namely, the self-shielding of the elastic transfer matrix elements is the same as that for the elastic cross section. It is possible that this assumption can lead to significant errors.

To explore this question elastic transfer cross sections were computed using MINX with the following flux:

$$\sigma(E) = \frac{1}{\sigma_t(E) + \sigma_0} \quad . \quad (1)$$

Table I shows self-shielding factors for ENDF/B-IV iron (MAT 1192) for a portion of a standard 50-group structure used for the CCCC 22-nuclide library. It is clear that substantial differences exist between downscatter and elastic self-shielding. Using the elastic f-factor to evaluate the elastic removal cross section will lead to large percentage errors in most groups.

5

TABLE I

ELASTIC SELF-SHIELDING FACTORS FOR IRON (MAT-1192)
FOR A PORTION OF THE STANDARD FIFTY GROUP STRUCTURE (σ_0 = 1 barn)

Group	Top Energy	Bottom Energy	Self-Shielding Factors		
			Elastic	In-group	Downscatter
7	8.208E + 05	4.979E + 05	.803	.806	.722
8	4.979E + 05	3.877E + 05	.842	.876	.695
9	3.877E + 05	3.020E + 05	.648	.629	.948
10	3.020E + 05	2.352E + 05	.781	.770	.849
11	2.352E + 05	1.832E + 05	.728	.764	.529
12	1.832E + 05	1.426E + 05	.729	.810	.458
13	1.426E + 05	1.111E + 05	.568	.544	.795
14	1.111E + 05	8.652E + 04	.939	1.003	.680
15	8.652E + 04	6.738E + 04	.467	.429	1.277
16	6.738E + 04	5.248E + 04	.946	1.003	.704
17.	5.248E + 04	4.087E + 04	.986	.996	.929
18	4.087E + 04	3.183E + 04	.945	1.011	.666
19	3.183E + 04	2.479E + 04	.241	.224	2.658
20	2.479E + 04	1.930E + 04	.935	.971	.778
21	1.930E + 04	1.503E + 04	.985	1.006	.857
22	1.503E + 04	1.171E + 04	.990	1.007	.883

Similar calculations were carried out at the supergroup level using group bounds from the standard 240-group structure.[24] Although the differences were mitigated, substantial effects remained. For example, for fine groups in coarse group 12, differences between elastic f-factors and in-group transfer as large as 25% were observed.

In summary, the use of elastic cross section self-shielding for elastic transfer can lead to significant errors, particularly in broad group structures. These results will be reported at the June meeting of the American Nuclear Society in a paper by R. E. MacFarlane and M. Becker entitled "Self-Shielding of Elastic Transfer Matrices."

E. MINX-II Development (R. E. MacFarlane and R. M. Boicourt)

For the last year, a new nuclear cross section processing code has been under development. This code uses the same basic approaches developed for MINX; it was originally intended to be more efficient than MINX and to add new processing capabilities to the parent code. Early studies of the MINX code showed that the major sources of inefficiency were data flow and BCD input/output. Neither of these problems could be readily solved in the existing structure of MINX. In addition, the structure of MINX was not well adapted to gamma production cross section processing. Therefore, it was found necessary to make major changes in the structure of the

code which have resulted in a complete rewrite of the program. Since the name MINX-II implies an evolution rather than a mutation, it has been decided to rename the code.

Henceforth, the new nuclear cross section processing system will be called NJOY. This name was obtained by moving each letter in MINX up one step; the name can be interpreted as meaning "MINX plus."

The basic structure of the NJOY nuclear cross section processing system is shown in Fig. 2. It consists of a set of modules which operate on data from a library or the outside world. The modules communicate with each other through disk or tape files only. This protects modules from interfering with each other, makes it easy to link modules in various sequences for special calculations, and allows new modules to be added with minimal effects on the existing coding.

The modules all have access to a set of basic service routines in the main overlay. These include input/output routines for ENDF/B formats which can be modified for optimum efficiency on a given computer without having to change the calculational modules. In some terminal-based operating systems, it may be advantageous to put these utility routines into a "program library" and link modules by commands from the terminal. The NJOY system would then give the operator maximum control and flexibility by putting him "in the loop."
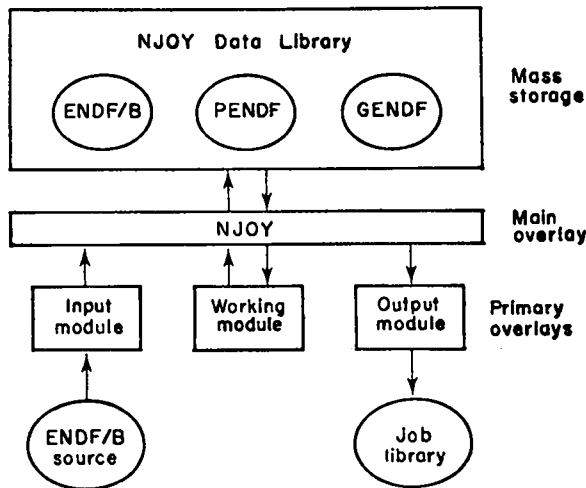
Fig. 2. Basic structure of NJOY nuclear data processing system (overlayed version).

The data library files are an important part of this system. The "point-wise ENDF/B" (PENDF) file is generated using detailed point reconstruction of resonances, the accurate but expensive kernel method for Doppler broadening resolved resonance peaks, and a sophisticated unresolved resonance calculation including overlap effects. This file has to be regenerated infrequently and is used as input for subsequent processing. The "group-wise ENDF/B" (GENDF) file stores group constants in an ENDF/B-like format using the histogram interpolation law. Using ENDF format assures that there is a slot for every reaction on the ENDF/B tape and takes advantage of much existing experience with the format. Existing utility codes can often be used with only minor changes. Once a GENDF tape has been generated it can be collapsed and formatted into a variety of specialized job libraries at very low cost.

The calculational path for generating a PENDF and a GENDF tape is shown in Fig. 3. The RECONR module reconstructs point resonance cross sections on a linearized and unionized grid using methods from RESEND,[25] MINX, and ETOPL.[26] The BROADR module Doppler broadens these cross sections using the method of SIGMA1[27] modified to operate at high temperatures. The UNRESR module adds self-shielded unresolved resonance cross sections to the PENDF tape. The GROUPR module computes neutron and gamma production group constants and formats them for GENDF. A typical subsequent processing step is shown in Fig. 4. The group constants from GENDF are collapsed to
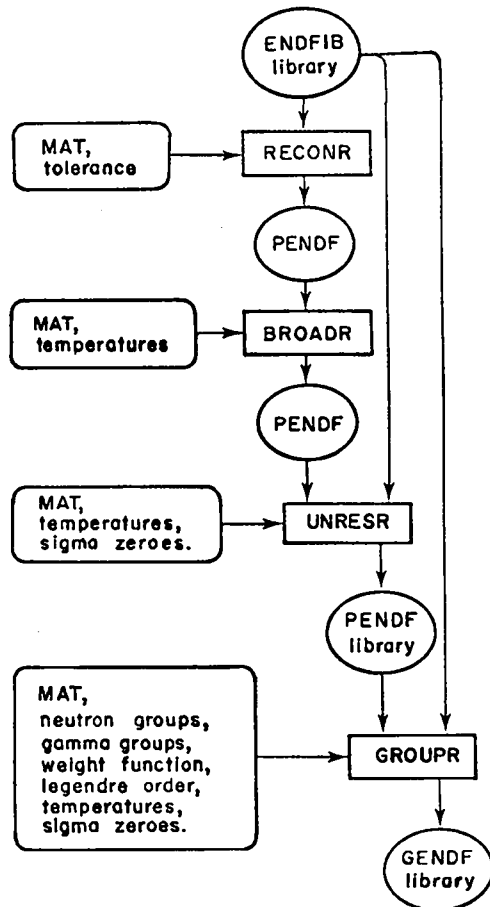
Fig. 3. Calculational path for generating PENDF and GENDF library files with NJOY.
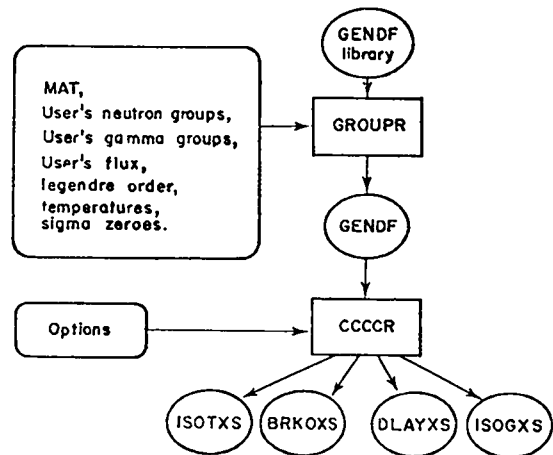
Fig. 4. Calculational path for collapsing to user specified group structure and flux and writing a job library in a specified format with NJOY

the user's group structure and flux using GROUPR, then converted to CCCC format.

7

The first phase of NJOY development is scheduled for completion in September of 1975. It will include the RECONR, BROADR, and UNRESR modules for generating PENDF library tapes (the UNRESR module will be a preliminary version using the ETOX method). The GROUPR module will be able to generate self-shielding neutron and gamma production cross sections including delayed neutrons. An input module called MODER will be provided to convert existing BCD and binary ENDF/B tapes into the special blocked binary format used in NJOY. And finally, the first phase will include the output modules CCCCR, SNR, and MCXR for CCCC, discrete ordinates, and continuous energy Monte Carlo job libraries.

Development this quarter has concentrated on the GROUPR module. It now possesses all allowed neutron reaction types and formats including delayed neutrons and all allowed gamma production formats except for the transition probability arrays. It does not write the GENDF output, and the binary input/output logic has not been activated. Gains in calculational efficiency have been obtained by introducing parallel data flows. For example, self-shielded group constant integrals are accumulated for all values of σ_0 simultaneously, and all Legendre orders and final energy groups for scattering matrices are integrated simultaneously. Additional gains are obtained by avoiding "over-kill." For example, reaction rates and fluxes are integrated using the trapezoidal method on the grid found on the PENDF tape. This is equivalent to an adaptive integration because the PENDF grid was chosen to represent the cross section to a specified accuracy.

The discrete channel scattering matrices require integration on a finer scale inside the panels defined by the PENDF grid. In MINX, this problem is solved by adaptive integration. However, it is possible to estimate the polynomial order of the integrand from the atomic weight ratio and various Legendre orders. This estimate enables NJOY to use a Gaussian quadrature formula which performs the integral with the theoretical minimum number of function evaluations. Since the evaluation of the argument of these particular integrals is very time-consuming, the use of such a fixed point quadrature scheme is much more efficient than adaptive integration. Furthermore, increased accuracy is obtained in many important cases because adaptive integration is not

well suited to functions which oscillate around zero. Representative efficiency improvements and accuracy comparisons are given in Table II.

An important goal in the restructuring of MINX was to reduce its size while improving its readability and maintainability. This has been achieved in NJOY by a generalization of the cross section processing process and a separation of well-defined portions of the calculation. The key to this generalization is the "feed function" — the total yield into a specified final energy group from a specified initial energy point. Using various forms of this function, all group cross sections and group-to-group transfer matrices for neutrons and gamma rays can be computed by the same integration routine. This is a great economy in coding. Each factor of the feed function is computed by a separate and independent subroutine. These retrieval routines are GETYLD for neutron yields, GETFLE for neutron angular distributions, GETSED for neutron and photon secondary energy distributions, GETGFL for photon angular distributions, and GETGYL for discrete and continuous photon yields. The integrals for the group constants also require the cross sections

TABLE II

COMPARISON OF RUN-TIME AND ACCURACY FOR REPRESENTATIVE CALCULATIONS USING MINX AND NJOY

Calculation Performed	MINX (CP seconds)	NJOY (CP seconds)	Maximum Difference
U-238 elastic self-shielded cross sections[a]	162.61	35.12	<0.5% typically <0.01%
U-235 elastic P_3 transfer matrix[b]	43.88	7.84	<0.1% below 5 MeV P_0 < 1% below 20 MeV
U-235 anisotropic discrete inelastic[b,c]	354.11	2.41	P_0 < 4% (or 8 x 10^{-5}b)
U-235, n2n, n3n, and continuum inelastic transfer matrices[b]	6.69	6.34	<1% typically <0.1%

[a] 50 groups, 4 temperatures, 6 dilutions.

[b] 30 groups, zero degrees, infinite dilutions.

[c] Given laboratory coefficients were used in the center-of-mass.

and fluxes; they are obtained using GETSIG and GETFLX. All input/output, paging, and storage complexities are handled by these routines (and the utility routines in the main overlay) and do not interfere with the logic and readability of the calculational algorithms. That this unified design approach does indeed lead to improvements in size is demonstrated in Table III. NJOY is heavily commented, but still manages to perform more functions than MINX and LAPHANO[28] combined with one-third as much coding.

The major new capability of NJOY is its ability to generate gamma-ray production cross sections and matrices. This capability offers three advances over LAPHANO:[28] the cross sections are consistent with the corresponding neutron cross sections, self-shielding cross sections can be computed explicitly, and anisotropic transfer matrices can be generated. The consistency of neutron and photon cross sections is obtained because both types of cross sections are obtained from the same data tape at the same time and integrated with the same routine using the same point weight function. Self-shielded cross sections can be computed explicitly using the same self-shielded flux used for the neutron cross sections. The usual practice of using the neutron f-factors is adequate when the photon yields are constant, but this is not always the case. The new code has been compared with LAPHANO results and with hand calculations. Where agreement is less than perfect, NJOY agrees with the exact hand calculations.

F. ETOPL and LAPHANO Code Development (R. J. La-Bauve and K. A. Hansborough)

The ETOPL[26] code is being updated to handle Version IV materials. This has required changes to the LUST and GAMADD routines to allow for new MT numbers. In the new version, the code will linearize, unionize, and thin all reactions given on the original ENDF/B tape. A simplification in ETOPL input specifications has also been made. The processing of 19 nuclides from ENDF/B-IV for a LASL TD-6 group PENDF library is now in progress with the new version of the ETOPL code.

Linking of the LAPHANO[28] code with group cross sections from the MINX code was begun. Comparisons are also being made between the LAPHANO code and gamma-ray production routines in ETOPL.

TABLE III

COMPARISON OF NUMBER OF SOURCE CARDS IN MINX, LAPHANO, AND NJOY

Code	Source cards
MINX	8000[a]
LAPHANO	2600
NJOY	2900[a]

[a]Includes only the equivalent portions of these two codes.

III. NUCLEAR DATA FOR HTGR SAFETY RESERACH

A. Data Processing (M. G. Stamatelatos, R. J. LaBauve, and J. Vigil [T-1])

The current route for generating multigroup cross sections for HTGR neutronic calculations was described previously and is summarized, for convenience, in Fig. 5.

To date, cross section sets for 300, 1200, and 3000 K were generated using the data-flow system of Fig. 5. Cross sections for 500, 800, 1700, and 2300 K are currently being generated.

Some code modification was performed on MC^2 (Ref. 29) and on GLEN[30] which previously did not allow for energy variation of absorber scattering cross sections in the thermal region. Although good in most instances, the constant scattering cross section approximation fails for absorbers like ^{135}Xe and ^{149}Sm, yielding very inaccurate results. The current version of GLEN permits energy variation in the absorber scattering cross sections whenever required through a special input flag. Also, the current GLEN version is no longer limited to four absorbers when thermal spectrum is read in. It can take any number of absorber isotopes.

A critical evaluation of the obtained multigroup cross sections as compared with other non-LASL sets (e.g., from GA) is currently in progress. A restricted analysis yields the following preliminary conclusions on the initial LASL cross sections:

1. Double heterogeneity effects on cross sections (especially particle self-shielding) have not yet been included. One level of heterogeneity (fuel stick-moderator) will be considere·' next in order to determine its effect essentially on the ^{232}Th cross sections.

ABOVE THERMAL
ENDF/B BASIC FILES → MC^2 → FINE-GROUP X-SEC → MC^2 → BROAD-GROUP X-SEC

THERMAL
ENDF/B BASIC FILES → MC^2 → FINE-GROUP ABSORBER X-SEC

PHYSICS PARAMETERS GRAPHITE → HEXSCAT → FINE-GROUP COHERENT SCAT. X-SEC GRAPHITE → GLEN → BROAD-GROUP X-SEC

PHYSICS PARAMETERS GRAPHITE → TOR → FINE-GROUP INCOHERENT SCAT. X-SEC GRAPHITE

JMBLFAT → BROAD-GROUP X-SEC DTF FORMAT
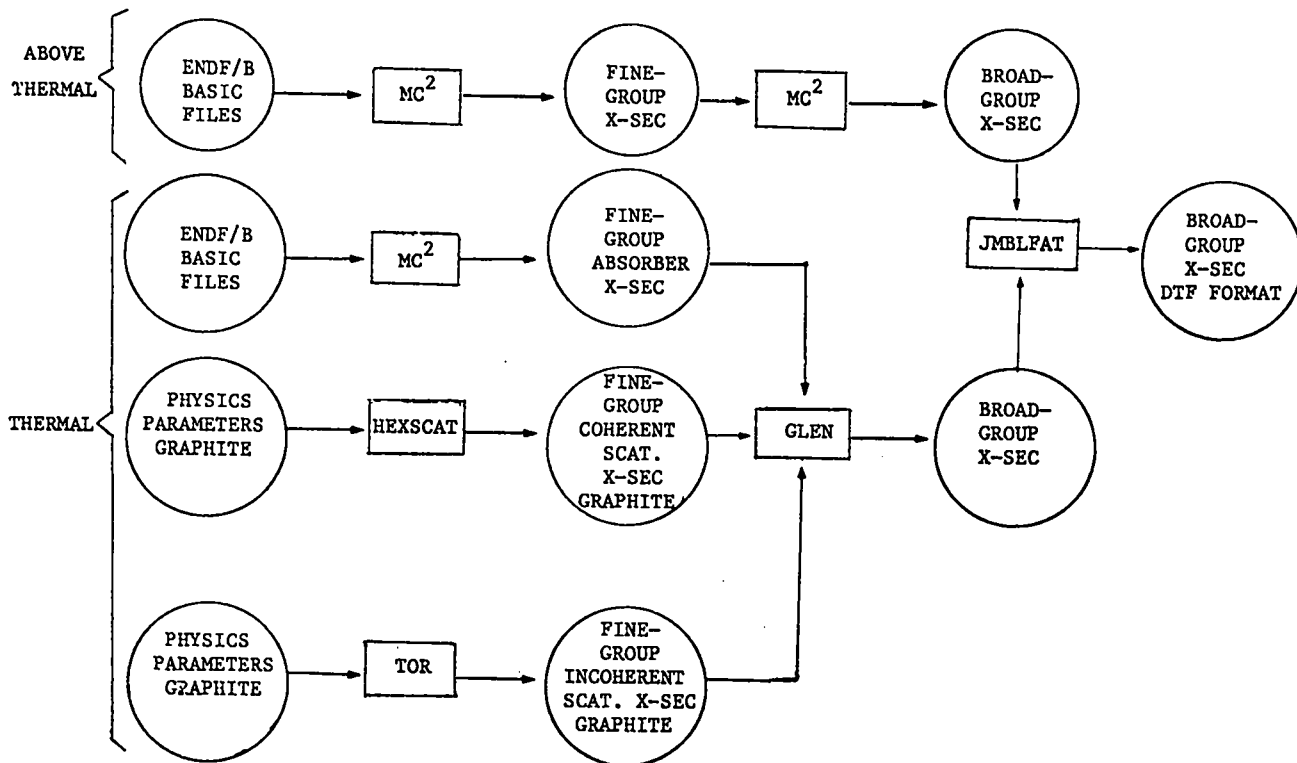
Fig. 5. Data flow for HTGR cross section generation.

2. Resonance absorber cross sections appear to be low especially in the resolved resonance region. This may be due to the relatively small number of energy groups used in the "all-fine" option of MC^2. "Ultra-fine" MC^2 runs with ~2000 energy groups in the above-thermal neutron region will be performed for comparison.

3. With some exceptions, thermal cross sections appear to be in reasonable agreement with the non-LASL set.

4. The variation of the ^{232}Th absorption cross section with temperature is slower than anticipated in the resonance region. Again, this may be due to the low number of energy grids used. It would be desirable to have a very fine energy grid resolution only in the resonance region. This, however, is not possible since MC^2 requires a uniform lethargy grid. As a consequence, MC^2 runs with very fine energy grid resolution in the entire above-thermal region must be carried out and they are time-consuming. In this connection, the use of MINX[31] using variable energy group size and other sophisticated techniques seems desirable. MINX runs

for at least one temperature are, consequently, planned for the immediate future. In addition, the possibility of comparison runs with MC^2-Version II (not yet operational at LASL) is anticipated, courtesy of the Argonne National Laboratory.

B. PHONEX (M. G. Stamatelatos)

PHONEX is a FORTRAN-IV computer program to calculate photoneutron spectra for arbitrary energy distributions of gamma rays incident upon specific elements or materials. The photon spectrum and the photoneutron cross section as a function of the photon energy are required as input. Knowledge of the functional dependence of the double-differential photoneutron cross section on the neutron angle in the center-of-mass system is also useful. All kinematic calculations are relativistic. The full details about the program can be found in Ref. 32.

C. GLEN Code Improvements (M. G. Stamatelatos, R. M. Boicourt, and R. J. LaBauve)

The GLEN[30] FORTRAN-IV computer program was developed to obtain thermal neutron scattering cross sections for transport calculations and to determine the diffusion length for thermalized neutrons. It

has been extensively used at LASL for generating multigroup cross sections in the thermal neutron region. The present discussion is addressed only to certain shortcomings of the code which have been recently eliminated.

In its original version, the code allows for a composition of one moderator material and of up to four non-moderating isotopes hereafter called "absorbers." This causes the user to be faced with a long and unnecessarily cumbersome procedure where he desires to include more than four absorbers into the mixture, as is often the case.

Up until now, the procedure has been to first run the program in the option NSPEC = 1 (calculating a fine-group neutron spectrum to be used for weighting in the multigroup process) with a mixture including the moderator and the four most important absorbers in the desired composition, i.e., those which most strongly determine the neutron spectrum. The fine-group neutron spectrum calculated in this run is provided in card form for input inclusion in subsequent runs each to be performed with the option NSPEC = -1 (which uses input fine-group spectrum for multigrouping) and with a mixture containing the moderator and up to four of the other less important absorbers. This procedure is followed for a total of N/4 runs (N is the total number of absorbers) until the broad-group cross section for all isotopes in the desired composition are obtained.

Also, relying on the fact that most non-moderating isotopes have scattering cross sections which are relatively small and relatively energy-independent in the thermal region, the original GLEN version allows for a single (average) scattering cross section value for each absorber. This limitation causes drastic errors in the treatment of resonant scattering materials with large scattering cross sections, e.g., ^{135}Xe and ^{149}Sm. This deficiency has been removed by including an option for each isotope (selected by the user through a flag, ISCAT) to either treat the absorber scattering cross section as in the original GLEN version or to treat it as energy-dependent as it is required by isotopes like ^{135}Xe and ^{149}Sm. In either case, the absorber scattering cross section, SIGSIS, must be read in; as a single number, when ISCAT = 0, or as an energy-dependent array, when ISCAT = 1.

With the new version it is possible to obtain, in a single GLEN computer run, broad-group cross sections for an isotope mixture containing one moderator and an arbitrary number, NISOMA, of absorbers without increasing computer-memory code requirements. This is achieved by running two versions of the GLEN code in tandem: first, with the option NSPEC = 1 in which a mixture of one moderator and up to four absorbers is treated and, next, a second version (to be used only in the option NSPEC = -1) for multigrouping the cross sections of the remaining absorbers.

The first part of the calculation yields the neutron spectrum and stores it on tape. It also gives broad-group cross sections for the moderator and the four most important absorbers. The second part of the calculation reads the neutron spectrum from tape and sequentially yields broad-group cross sections for the remaining absorbers.

As a note of caution, it should be pointed out that, if the two GLEN calculations are to be executed in the order described above, NSPEC must be set equal to 1 in the first part of the calculations and -1 in the second part, as indicated.

D. Reference Decay Energies and Yields (T. R. England and N. L. Whittemore)

At GA's request for a reference set of decay data for use in, e.g., dose calculations, the average β and γ energies, half-lives, branching fractions, and decay modes in Table IV were supplied. Data for the listed nuclides were specifically requested. These data are processed from ENDF/B-IV files. In addition, a complete listing of ENDF/B-IV independent fission yield data processed into a readable format, and cumulative yields for the nuclides listed in Table IV were sent to GA (R. K. Deremer).

In response to a separate request, the CINDER code plus libraries for decay heat and absorption calculations were also sent to GA (F. Dombeck). These data are not ENDF/B-IV.

IV. NUCLEAR DATA FOR CTR APPLICATIONS

A. Effect of Multigroup Energy Widths on Neutron Transport Results (J. M. Wallace [TD-1], D. W. Muir, and W. A. Reupke)

The neutronic analysis of fusion reactor integral experiments requires an evaluation of the impact of different choices of calculational parameters (e.g., Legendre order, quadrature, spatial mesh size)

TABLE IV

SELECTED DECAY DATA

NUCLIDE	HALFLIFE	TYPE OF DECAY	BRANCHING RATIOS		E-BETA	E-GAMMA
KR-83M	6.6960+03	3	1.0		0.	4.1800+04
KR-85	3.3861+08	1	1.0		2.5059+05	2.2300+03
KR-85M	1.6128+04	1-3	7.88-01	2.12-01	2.2608+05	1.8322+05
KR-87	4.5600+03	1	1.0		1.3345+06	7.9260+05
KR-88	1.0080+04	1	1.0		2.4858+05	2.2118+06
RB-88	1.0620+03	1	1.0		2.0826+06	6.7392+05
RB-89	9.1200+02	1	1.0		9.2934+05	2.2890+06
RB-90	1.6200+02	1	1.0		1.6589+06	2.6604+06
KR-90	3.2300+01	1-1	8.40-01	1.60-01	1.1870+06	1.7491+06
KR-91	8.7000+00	1	1.0		2.5778+06	7.2356+05
SN-127	7.6320+03	1	1.0		6.7455+05	1.4343+06
SN-127M	2.4800+02	1	1.0		1.1342+06	4.9400+05
SB-127	3.2832+05	1-1	8.40-01	1.60-01	3.1806+05	6.4432+05
TE-127	3.3660+04	1	1.0		2.2728+05	5.1700+03
TE-127M	9.4176+06	1-3	2.40-02	9.76-01	4.9793+03	9.1865+04
SN-129	4.5000+02	1	1.0		1.1452+06	1.3847+06
SN-129M	1.5000+02	1	1.0		1.2164+06	1.4708+06
SB-129	1.5624+04	1-1	7.60-01	2.40-01	3.5911+05	1.3010+06
I-129	5.0142+14	1	1.0		6.2400+04	4.0000+04
TE-129	4.2000+03	1	1.0		5.3394+05	7.2900+04
TE-129M [a]	2.8858+06	1-3	3.66-01	6.34-01	2.1402+05	2.9800+04
SN-131	6.3000+01	1	1.0		1.3054+06	1.7069+06
SB-131	1.3800+03	1-1	9.32-01	6.80-02	7.1369+05	1.7025+06
I-131	6.9474+05	1-1	9.93-01	7.00-03	1.8550+05	3.8928+05
TE-131	1.5000+03	1	1.0		6.7172+05	4.2280+05
TE-131M	1.0800+05	1-3	8.20-01	1.80-01	1.8218+05	1.4911+06
XE-131M	1.0359+06	3	1.0		0.	1.6754+05
I-132	8.2260+03	1	1.0		5.2468+05	2.2377+06
TE-132	2.8080+05	1	1.0		6.0050+04	2.6860+05
SN-132	4.0000+01	1	1.0		6.6029+05	1.3228+06
SB-132	1.2600+02	1	1.0		1.7221+06	2.0066+06
I-133	7.4880+04	1-1	8.60-01	1.40-01	4.1718+05	5.9890+05
SB-133	1.4400+02	1-1	9.776-1	2.24-02	5.3711+05	3.1625+06
TE-133	7.5000+02	1	1.0		8.1997+05	9.8324+05
TE-133M	3.3240+03	1-3	8.70-01	1.30-01	5.5207+05	1.8661+06
XE-133	4.5706+05	1	1.0		1.0188+05	8.1440+04
XE-133M	1.9267+05	3	1.0		0.	2.3269+05
XE-135	3.3012+04	1	1.0		3.0989+05	2.6143+05
XE-135M	9.1800+02	3	1.0		0.	5.2682+05
I-135	2.3706+04	1-1	8.53-01	1.47-01	3.9365+05	1.4560+06
CS-135	7.2533+13	1	1.0		6.9400+04	1.0000+02
XE-137	2.3040+02	1	1.0		1.8407+06	1.9526+05
XE-138	8.5200+02	1	1.0		6.5770+05	1.1951+06
XE-139	4.0400+01	1	1.0		1.7868+06	9.2749+05
XE-140	1.3600+01	1	1.0		8.8074+05	1.3624+06
CS-140	6.3800+01	1	1.0		1.9312+06	2.1310+06
BA-140	1.1051+06	1	1.0		2.8027+05	2.1687+05
LA-140	1.4483+05	1	1.0		5.1701+05	2.2048+06
PR-144	1.0368+03	1	1.0		1.2628+06	3.1010+04

KEY
    DECAY MODE
       1 - BETA
       3 - IT

[a] A conversion electron energy of ~0.071 MeV is not included for TE-129M

on the calculated results. For example, a previous analysis[33] of a tritium-production measurement[34] in LiD showed that a $S_{16}P_1$ calculation predicted a ^7Li tritium-production rate up to 13% higher than a corresponding $S_{16}P_3$ calculation. One calculational parameter not varied in Ref. 33 is the coarseness of the multigroup energy structure. We have now examined this effect by performing neutron transport calculations using fewer energy groups (10 and 21) than the previous study (100 groups), as well as continuous-energy Monte Carlo, which is equivalent to using an infinite number of groups.

Multigroup (S_n) and Monte Carlo (M.C.) results for a simple test problem are compared. The problem consists of a spherical shell of ^6LiD, with an outer radius 12.6 cm, inner radius 2.2 cm, and density 0.77 g/cm^3. Neutrons are introduced isotropically at the center of the system.

Three S_n runs were made: (1) a 10-group S_4P_1 run with source energy bin 13.5-17.0 MeV, using LS_n;[35] (2) a 21-group S_8P_1 run with source energy bin 13.5-15.0 MeV, using LSN; (3) a 100-group $S_{16}P_3$ run with source energy bin 13.5-14.92 MeV, using DTF-IV.[36] A M.C. run with source energy bin 13.5-14.9 MeV was made using MCN.[37] For all calculations the Li cross sections are based on ENDF/B-III and the D cross sections are based on a LASL evaluation.[38]

The leakage spectra (normalized to a unit neutron source) from the four calculations are compared in Table V. The general agreement between the M.C. and 100-group S_n calculations is very good, the differences averaging around 3% for energy bins above 0.2 MeV. Thus, for most problems of this type, 100 groups can be considered entirely adequate. The 21-group S_n results are generally closer to the M.C. calculation than the 10-group S_n results. The S_n calculations thus appear to be converging to the M.C. results in a reasonable manner. The energy-integrated leakage spectra for the four calculations agree within 4%.

B. Fast Neutron Data Testing (D. W. Muir)

A program has been initiated to test processed cross sections against integral experiments involving high-energy (usually 14-MeV) neutron sources. As part of this program, we have assembled a code system which incorporates most of the relevant neutron transport codes as modules. This code system utilizes a driver program to construct CROS control card decks required for a particular transport code, the code being selected by a single input data card. UPDATE decks for the transport codes are stored in PHOTOSTORE, while the driver program itself resides on hydra disk, in order to facilitate revisions and extensions of the driver. The code system, called EZTRAN, currently contains as modules the discrete ordinates transport codes DTF[36] and TWOTRAN,[39] as well as the multigroup Monte Carlo codes MCMG[40] and ANDY.[41] Pointwise Monte Carlo capability will be added in the near future.

We also plan to modify the various transport code input routines in order to increase the compatibility of the formats required for cross section libraries and problem specification data. In this development work, a useful feature of the driver program is that the UPDATE deck for the transport code selected is automatically revised in PHOTOSTORE (as a new version of that file), if the user requests that option on the EZTRAN input data card.

V. VALIDATION OF SENSITIVITY PROFILES (D. R. Harris and W. B. Wilson)

The sensitivity profile displays the differential change in a flux-integrated response for a differential change in nuclear data. We have previously examined the mathematical development of sensitivity theory and its employment in the selection of multigroup structure.[42] We now wish to investigate the accuracy of the sensitivity profile, as calculated from linear perturbation theory, by considering neutron transport in an iron shield.

The shield consists of a 70-cm-radius sphere of iron with a 4-cm-radius void at the center. The isotropic neutron source is uniformly distributed in a central 1-cm-radius sphere and has the 0° spectrum of neutrons produced by 50-MeV deuterons on beryllium.[43] The response quantity consists of the product of the neutron flux and neutron fluence-to-dose equivalent factor summed over all neutron energy groups and averaged over the volume of the 1-cm-thick air shell at the outer surface of the sphere.[44]

The DTF neutron transport code[36] was used to calculate the neutron fluxes and adjoint fluxes throughout the shield, using 41-group P_5 cross sections and S_{16} quadrature. The source for the adjoint calculation, located in the 1-cm-thick shell surrounding the sphere, was the vector of neutron fluence-to-dose equivalent conversion factors.

TABLE V

LEAKAGE SPECTRA

E_{MAX} (MeV)	10-GROUP S_4P_1	NO. OF GROUPS IN BIN	21-GROUP S_8P_1	NO. OF GROUPS IN BIN	100-GROUP $S_{16}P_3$	NO. OF GROUPS IN BIN	M.C.
17.00	0.328	1	0.360	2	0.364	1	0.375 ± 0.001
13.50	0.180	1	0.189	2	0.169	3	0.172 ± 0.001
10.00	0.0584	1	0.0569	1	0.0546	2.5	0.0541 ± 0.0004
7.79	0.0937	1	0.103	2	0.0996	7.5	0.1008 ± 0.0005
3.68	0.0570	1	0.0542	2	0.0480	5	0.0472 ± 0.0004
2.23	0.104	1	0.105	4	0.0975	15	0.0962 ± 0.0005
0.50	0.0242	1	0.0245	2	0.0228	10	0.0218 ± 0.0002
0.184	0.0560	1	0.0530	2	0.0519	11	0.0508 ± 0.0003
0.0248	0.0200	1	0.0180	2	0.0178	8	0.0169 ± 0.0002
-0.00335							
SUM	0.921		0.964		0.925		0.935 ± 0.002

The ALVIN code was used to produce the sensitivity profile histogram shown in Fig. 6, showing the sensitivity of the neutron dose equivalent rate at the shield surface to the cross section data. The ALVIN calculation uses first-order perturbation theory; this approximation, as well as code accuracy, can be validated by comparison with reference calculations.

The reference approach to determine the change in the result due to a change in the cross section data involves the creation of an altered cross section set, performing a neutron transport calculation using the altered cross sections, and converting the fluxes in the outer shell to the neutron dose equivalent rate. The fractional change in the dose equivalent rate divided by the fractional change in the cross sections of group IG thus yields the sensitivity P(IG) of the result to cross sections in group IG.

Sixteen separate altered cross section sets were formed with $\Sigma_T(IG)$ and $\Sigma^\ell(IG \rightarrow IG')$, $IG' = IG, NG$ for all ℓ increased by 0.1, 0.5, 1.0, or 10.0% for groups IG = 9, 19, 20, or 25. The sensitivities resulting from the neutron transport calculations are superimposed on the sensitivity profile histogram of Fig. 6. The separate DTF calculations were con-

verged to 10^{-4}, so only those directly calculated sensitivities are shown for which the relative change in dose equivalent exceeded 10^{-4}. For example, the dose equivalent changed from 0.7189×10^{-13} rem/s to 0.7188×10^{-13}, 0.7187×10^{-13}, and 0.7186×10^{-13} rem/s when the cross sections of group 19 were increased by 0.1, 0.5, and 1.0%, respectively. Therefore, these cases were disregarded.

In addition to accuracy problems in the direct calculations, there are nonlinearity problems in the perturbation calculation. Consider monoenergetic neutron penetration through a slab of thickness X with cross section Σ. Then

$$P_{direct} = -\left[1 - \frac{1}{2!} X\Sigma \frac{\delta\Sigma}{\Sigma} + \frac{1}{3!} \left(X\Sigma \frac{\delta\Sigma}{\Sigma} \right)^2 - \ldots \right] X\Sigma \quad . (2)$$

If $\delta\Sigma/\Sigma$ is chosen to be 0.1 in order to insure accuracy in the dose equivalent change, then for the shield thickness studied here (about 12 mean free paths thick) the direct calculation underpredicts the result for very small $\delta\Sigma/\Sigma$ by about one-third according to Eq. (2). This nonlinear effect is observed in Fig. 6.
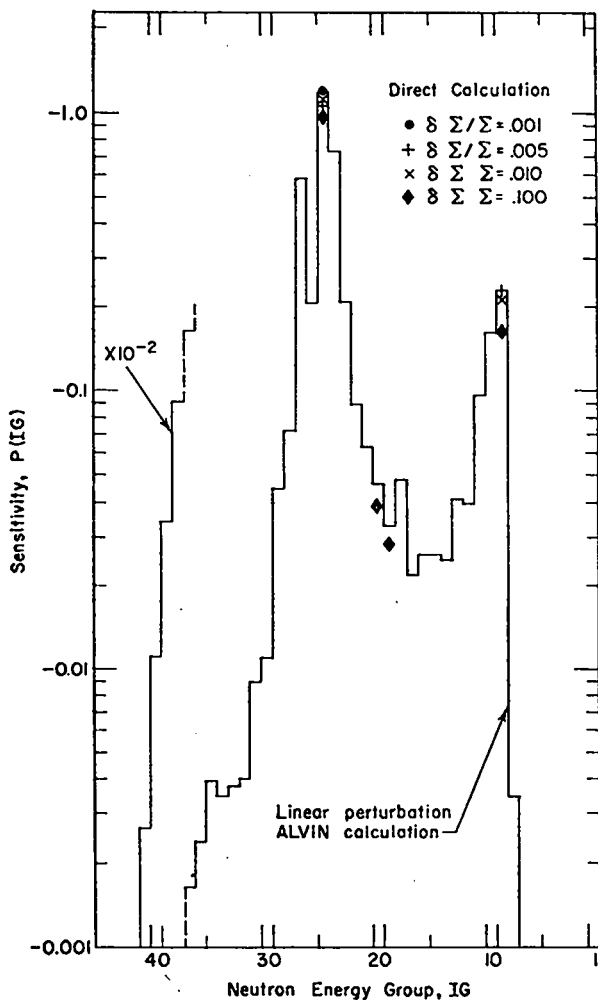
Fig. 6. Sensitivity of shield surface neutron dose equivalent rate to neutron cross section data computed by direct change in cross sections and by linear perturbation ALVIN calculation.

VI. FISSION-PRODUCT YIELD AND RADIOACTIVE DECAY STUDIES

A. ENDF/B Fission-Product Yields (T. R. England and N. L. Whittemore)

A yield processing code was modified to list the 11 313 independent yields in ENDF/B-IV in a readable format for use in a joint LASL/HEDL documentation report.

Extensive new fast reactor fission yields for ^{233}U, ^{235}U, ^{238}U, and ^{239}Pu have recently been reported. ENDF/B-IV does not contain ^{233}U fast yields. For the three remaining sets, Tables VI, VII, and VIII compare the new data with the ENDF/B-IV evaluations, including uncertainties. (Reference 45 notes that the ^{239}Pu values are still preliminary.)

These new data generally have smaller assigned uncertainties than ENDF/B-IV; for this reason, they have been used in repeating the delayed neutron calculations (see Sec. VI, F). The resulting changes in ν_d are not significant.

Various yield weighted quantities using the final ENDF/B-IV files are listed in Table IX. It should be noted, in particular, that the fissile nuclide charge is nearly conserved. Values in column four can be used to estimate prompt neutron yields and the last column indicates the average number of β decays per isobaric chain (e.g., $Z_f - \bar{Z} =$ 6.08 for ^{235}U). All 10 yield sets sum to 2.0000.

B. ENDF/B Decay Parameters and Cross Sections (T. R. England and N. L. Whittemore)

A code was prepared to process the parameters most often requested by users (half-lives, branching fractions, decay modes, average β, γ, and α decay energies, σ_{2200} and resonance integrals, activation fractions, etc.). This table of data is very compact and includes data for all 824 nuclides in the ENDF/B-IV fission product files. It will be included in a joint LASL/HEDL documentation report of the new files.

A tape containing average β and γ decay energies in the CINDER-10 format has been prepared and a copy will be sent to the Bettis Atomic Power Laboratory following a test of the current coding.

C. CINDER Code Development (T. R. England, N. L. Whittemore, and R. Wilczynski [Bettis Atomic Power Laboratory])

1. CINDER-7. A report for users of this version was prepared.[46] Some additional improvements in roundoff algorithms are still in progress and will be incorporated into CINDER-10. Version 7 of CINDER provides extended calculational features over earlier versions, e.g., free form data formats, etc., as described in previous progress reports.

2. CINDER-10. This version of CINDER required extensive debugging effort during this quarter. It retains the features of Version 7 while eliminating the redundant I/O previously required for linear nuclide chains. ENDF/B-IV data is being processed into the format required for this version.

D. Decay Heat Calculations (T. R. England and N. L. Whittemore)

Preliminary calculations of the β and γ decay heating rates expected in short term irradiation of

TABLE VI

COMPARISON OF CUMULATIVE ENDF/B-IV YIELDS WITH REF. 45
^{235}U FISSION SPECTRUM

	PERCENT YIELD REF 45	UNCERTAINTY		PERCENT YIELD ENDF/B-IV	UNCERTAINTY
75- 80	0.24		75- 80	0.302	
81	0.22	+/-0.05	81	0.236	+/-0.054
82	0.36	+/-0.09	82	0.322	+/-0.074
83	0.569	+/-0.005	83	0.576	+/-0.008
84	1.03	+/-0.01	84	1.025	+/-0.014
85	1.35	+/-0.01	85	1.308	+/-0.013
86	1.96	+/-0.02	85	1.308	+/-0.013
87	2.57	+/-0.02	87	2.415	+/-0.048
88	3.51	+/-0.03	88	3.586	+/-0.072
89	4.51	+/-0.23	89	4.562	+/-0.128
90	5.52	+/-0.04	90	5.572	+/-0.111
91	5.50	+/-0.05	91	5.591	+/-0.112
92	5.79	+/-0.05	92	5.724	+/-0.114
93	6.18	+/-0.06	93	6.096	+/-0.122
94	6.23	+/-0.06	94	6.187	+/-0.124
95	6.42	+/-0.06	95	6.383	+/-0.064
96	6.13	+/-0.06	96	6.087	+/-0.122
97	5.99	+/-0.05	97	5.960	+/-0.083
98	5.91	+/-0.05	98	5.869	+/-0.082
99	6.15	+/-0.31	99	5.701	+/-0.080
100	6.39	+/-0.06	100	6.245	+/-0.087
101	5.24	+/-0.24	101	5.420	+/-0.108
102	4.41	+/-0.20	102	4.593	+/-0.092
103	3.25	+/-0.22	103	3.290	+/-0.065
104	2.09	+/-0.10	104	2.312	+/-0.046
105	1.32	+/-0.08	105	1.152	+/-0.046
106	0.547	+/-0.025	106	0.575	+/-0.035
107	0.17	+/-0.04	107	0.377	+/-0.060
108	0.08	+/-0.02	108	0.208	+/-0.023
109-116	0.16		109-116	0.408	
117-124	0.14		117-124	0.312	
125	0.038	+/-0.004	125	0.077	+/-0.006
126	0.071	+/-0.009	126	0.144	+/-0.016
127	0.151	+/-0.019	127	0.312	+/-0.034
128	0.372	+/-0.050	128	0.691	+/-0.076
129	0.840	+/-0.107	129	1.041	+/-0.083
130	1.71	+/-0.21	130	1.918	+/-0.153
131	3.18	+/-0.02	131	3.232	+/-0.045
132	4.60	+/-0.03	132	4.654	+/-0.065
133	6.82	+/-0.05	133	6.471	+/-0.091
135	6.52	+/-0.05	135	6.276	+/-0.126
136	6.16	+/-0.04	136	6.245	+/-0.062
137	6.21	+/-0.05	137	6.159	+/-0.062
138	6.66	+/-0.06	138	6.468	+/-0.091
139	6.76	+/-0.07	139	6.327	+/-0.044
140	6.19	+/-0.05	140	6.020	+/-0.084
141	5.85	+/-0.35	141	5.995	+/-0.120
142	5.78	+/-0.05	142	5.459	+/-0.153
143	5.80	+/-0.05	143	5.698	+/-0.057
144	5.27	+/-0.04	144	5.268	+/-0.074
145	3.83	+/-0.03	145	3.749	+/-0.037
146	2.94	+/-0.02	146	2.896	+/-0.029
147	2.11	+/-0.02	147	2.369	+/-0.066
148	1.68	+/-0.02	148	1.685	+/-0.012
149	1.02	+/-0.01	149	1.091	+/-0.031
150	0.672	+/-0.008	150	0.687	+/-0.010
151	0.406	+/-0.004	151	0.437	+/-0.009
152	0.265	+/-0.005	152	0.299	+/-0.006
153	0.168	+/-0.009	153	0.201	+/-0.016
154	0.072	+/-0.001	154	0.089	+/-0.005
155-160	0.07		155-160	0.113	

TABLE VII

COMPARISON OF CUMULATIVE ENDF/B-IV YIELDS WITH REF. 45
^{239}Pu FISSION SPECTRUM

	PERCENT YIELD REF 45	UNCERTAINTY		PERCENT YIELD ENDF/B-IV	UNCERTAINTY
75-80	0.22		75- 80	0.140	
81	0.16	+/-0.01	81	0.084	+/-0.019
82	0.23	+/-0.02	82	0.144	+/-0.033
83	0.309	+/-0.002	83	0.355	+/-0.010
84	0.490	+/-0.002	84	0.540	+/-0.022
85	0.595	+/-0.006	85	0.635	+/-0.018
86	0.777	+/-0.004	86	0.850	+/-0.034
87	1.03	+/-0.01	87	1.110	+/-0.031
88	1.31	+/-0.02	88	1.378	+/-0.039
89	1.67	+/-0.09	89	1.820	+/-0.073
90	2.02	+/-0.02	90	2.128	+/-0.060
91	2.48	+/-0.04	91	2.469	+/-0.069
92	3.02	+/-0.004	92	2.995	+/-0.084
93	3.80	+/-0.05	93	3.766	+/-0.105
94	4.28	+/-0.05	94	4.232	+/-0.118
95	4.71	+/-0.06	95	4.742	+/-0.095
96	4.84	+/-0.07	96	4.903	+/-0.137
97	5.33	+/-0.06	97	5.226	+/-0.105
98	5.66	+/-0.07	98	5.568	+/-0.156
99	6.09	+/-0.33	99	5.869	+/-0.164
100	6.64	+/-0.05	100	6.485	+/-0.182
101	6.54	+/-0.11	101	6.548	+/-0.183
102	6.64	+/-0.10	102	6.643	+/-0.186
103	6.05	+/-0.92	103	6.710	+/-0.134
104	6.53	+/-0.09	104	6.498	+/-0.182
105	5.43	+/-0.39	105	5.006	+/-0.400
106	4.32	+/-0.09	106	4.529	+/-0.362
107	3.41	+/-0.43	107	3.041	+/-0.335
108	2.40	+/-0.31	108	2.209	+/-0.243
109	1.51	+/-0.19	109	1.648	+/-0.099
110-118	1.52		110-118	1.712	
119-124	0.29		119-124	0.448	
125	0.125	+/-0.012	125	0.189	+/-0.021
126	0.27	+/-0.03	126	0.276	+/-0.044
127	0.52	+/-0.07	127	0.641	+/-0.071
128	0.95	+/-0.08	128	0.798	+/-0.128
129	1.61	+/-0.12	129	1.419	+/-0.156
130	2.54	+/-0.18	130	2.307	+/-0.254
131	3.84	+/-0.06	131	3.974	+/-0.079
132	5.27	+/-0.09	132	5.287	+/-0.148
133	6.99	+/-0.04	133	6.723	+/-0.134
134	7.39	+/-0.10	134	7.162	+/-0.286
135	7.57	+/-0.03	135	7.335	+/-0.205
136	6.99	+/-0.09	136	6.891	+/-0.276
137	6.61	+/-0.04	137	6.389	+/-0.128
138	6.12	+/-0.04	138	6.334	+/-0.253
139	5.51	+/-0.09	139	5.762	+/-0.346
140	5.39	+/-0.06	140	5.319	+/-0.074
141	5.15	+/-0.16	141	5.564	+/-0.223
142	4.89	+/-0.04	142	4.824	+/-0.135
143	4.37	+/-0.03	143	4.372	+/-0.061
144	3.70	+/-0.03	144	3.620	+/-0.072
145	3.01	+/-0.02	145	3.029	+/-0.042
146	2.46	+/-0.02	146	2.507	+/-0.035
147	1.99	+/-0.02	147	2.064	+/-0.124
148	1.65	+/-0.02	148	1.693	+/-0.024
149	1.23	+/-0.02	149	1.326	+/-0.027
150	0.981	+/-0.011	150	1.022	+/-0.014
151	0.776	+/-0.011	151	0.818	+/-0.023
152	0.589	+/-0.007	152	0.665	+/-0.019
153	0.444	+/-0.030	153	0.412	+/-0.045
154	0.264	+/-0.003	154	0.316	+/-0.009
155-160	0.53		155-160	0.600	

TABLE VIII

COMPARISON OF CUMULATIVE ENDF/B-IV YIELDS WITH REF. 45
^{238}U FISSION SPECTRUM

	PERCENT YIELD REF 45	UNCERTAINTY		PERCENT YIELD ENDF/B-IV	UNCERTAINTY
75- 80	0.1	+/-0.03	75- 80	0.078	+/-0.012
81	0.15	+/-0.04	81	0.127	+/-0.029
82	0.25	+/-0.06	82	0.255	+/-0.059
83	0.395	+/-0.004	83	0.377	+/-0.060
84	0.816	+/-0.008	84	0.753	+/-0.083
85	0.74	+/-0.01	85	0.758	+/-0.061
86	1.28	+/-0.01	86	1.195	+/-0.096
87	1.61	+/-0.02	87	1.523	+/-0.168
88	1.96	+/-0.05	88	2.292	+/-0.252
89	2.59	+/-0.14	89	2.975	+/-0.179
90	3.21	+/-0.05	90	3.354	+/-0.268
91	4.44	+/-0.27	91	3.874	+/-0.155
92	4.95	+/-0.29	92	4.211	+/-0.338
93	5.26	+/-0.31	93	4.843	+/-0.533
94	5.03	+/-0.30	94	4.527	+/-0.724
95	4.94	+/-0.08	95	5.324	+/-0.149
96	6.05	+/-0.36	96	5.292	+/-0.847
97	5.47	+/-0.06	97	5.530	+/-0.155
98	5.82	+/-0.07	98	5.554	+/-0.611
99	6.23	+/-0.32	99	6.247	+/-0.175
100	6.63	+/-0.08	100	6.133	+/-0.491
101	6.14	+/-0.36	101	6.579	+/-0.724
102	6.40	+/-0.38	102	6.792	+/-0.747
103	5.70	+/-0.38	103	6.336	+/-0.177
104	5.02	+/-0.30	104	5.437	+/-0.598
105	3.75	+/-0.29	105	4.210	+/-0.253
106	2.48	+/-0.16	106	2.752	+/-0.220
107	1.25	+/-0.31	107	1.272	+/-0.140
108	0.6	+/-0.15	108	0.623	+/-0.100
109-117	0.75	+/-0.19	109-117	0.754	+/-0.035
118-124	0.214	+/-0.054	118-124	0.262	+/-0.016
125	0.039	+/-0.004	125	0.054	+/-0.012
126	0.055	+/-0.007	126	0.070	+/-0.008
127	0.10	+/-0.01	127	0.130	+/-0.010
128	0.41	+/-0.05	128	0.509	+/-0.056
129	0.97	+/-0.13	129	1.111	+/-0.089
130	1.84	+/-0.24	130	1.776	+/-0.195
131	3.21	+/-0.03	131	3.213	+/-0.062
132	5.16	+/-0.03	132	5.029	+/-0.101
133	6.70	+/-0.06	133	6.357	+/-0.178
134	7.95	+/-0.05	134	7.099	+/-0.284
135	6.92	+/-0.06	135	6.563	+/-0.394
136	7.07	+/-0.05	136	6.011	+/-0.120
137	5.99	+/-0.05	137	6.194	+/-0.248
138	5.73	+/-0.17	138	5.960	+/-0.358
139	5.94	+/-0.14	139	6.110	+/-0.122
140	5.92	+/-0.12	140	5.889	+/-0.118
141	5.31	+/-0.16	141	5.143	+/-0.411
142	4.69	+/-0.04	142	4.931	+/-0.296
143	4.56	+/-0.04	143	4.834	+/-0.097
144	4.48	+/-0.04	144	4.751	+/-0.133
145	3.76	+/-0.03	145	3.998	+/-0.080
146	3.40	+/-0.04	146	3.610	+/-0.072
147	2.52	+/-0.03	147	2.711	+/-0.108
148	2.08	+/-0.03	148	2.259	+/-0.063
149	1.59	+/-0.02	149	1.765	+/-0.071
150	1.25	+/-0.02	150	1.362	+/-0.027
151	0.794	+/-0.019	151	0.854	+/-0.051
152	0.521	+/-0.005	152	0.557	+/-0.033
153	0.367	+/-0.019	153	0.412	+/-0.033
154	0.213	+/-0.004	154	0.230	+/-0.018
155-160	0.27	+/-0.07	155-160	0.266	+/-0.023

TABLE IX

SELECTED YIELD WEIGHTED QUANTITIES

Nuclide	$\sum_{i} y_i Z_i$	$\sum_{j} Y_j MS_j$	$\sum_{i} y_i N_i$	$\sum_{i} y_i A_i$	$\sum_{j} Y_j AS_j$	$\sum_{j} Y_j ZS_j$
U235T	92.0077	233.411	141.589	233.597	233.597	98.0818
U235F	92.0148	233.447	141.618	233.633	233.633	98.0840
U235HE	92.0731	232.257	140.371	232.444	232.444	97.6128
U238F	92.0298	236.143	144.299	236.329	236.329	99.2165
U238HE	92.0704	234.861	142.977	235.047	235.047	98.6443
PU239T	94.0148	236.906	143.077	237.092	237.092	99.4858
PU239F	94.0053	237.047	143.228	237.234	237.234	99.5331
PU241T	94.0054	238.822	145.003	239.009	239.009	100.2660
U233T	92.0027	231.346	139.529	231.532	231.532	97.2075
TH232F	90.0134	230.443	140.614	230.628	230.628	96.8762

Key: i denotes a sum over directly yielded nuclides.

j denotes a sum over mass numbers j.

y_i = direct yield.

Y_j = cumulative mass yield.

Z_i = charge of direct yield nuclide.

ZS_j = most stable charge, mass j.

AS_j = atomic number of most stable charge

MS_j = mass of most stable charge.

[235]U samples were made for use in planning aspects of the LASL group P-2 decay heat experiment.

E. Fallout Irradiation Following a [235]U and [239]Pu Fission Burst (T. R. England, R. E. Schenter [HEDL], and N. L. Whittemore)

Calculations of the β and γ intensities following a fission "burst" (1 s duration, and energy release rates calculated from 1 to 10^7 s) were made using ENDF/B-IV data. Separate calculations of the activity component due to gases were also made.

Preliminary results for the total and non-gaseous energy release rates are listed in Tables X and XI. Values below ~10 s are expected to be significantly low.

F. Delayed and Prompt Neutron Calculations Using ENDF/B-IV Data (T. R. England and N. L. Whittemore)

ENDF/B-IV yield and neutron emission probabilities have been used to calculate the delayed (ν_d) and prompt (ν_p) neutron emission for fission. The ν_d results are particularly sensitive to the yield vs charge dispersion, and the calculations are being used as a gross indication of needed improvement in the yield dispersion model to be used for ENDF/B-V.

Previously, calculations with and without a $\pm25\%$ even-odd Z effect using a pre-ENDF/B-IV yield compilation were reported in earlier progress reports; these indicated that ν_d was significantly im-

proved in magnitude and in energy dependence if the effect was removed from the dispersion model, particularly for fission spectrum and 14-MeV neutron energies.

Table XII compares the total ν_d and ν_p calculated values using the final ENDF/B-IV files with ENDF/B-IV evaluations.

Some 57 nuclides in the files are delayed neutron precursors. Tables XIII through XVII list the calculated contributions of each precursor in decreasing order for five of the fission yield sets. The group number is the approximate assignment of each nuclide, based on its half-life, to the standard six group structure.

The deviation of the calculated ν_d values from ENDF/B-IV evaluations could be due to several factors, including the cumulative chain yields. However, the new accurate fission spectrum yield measurements (Tables VI, VII, VIII) reported in Ref. 45 have been used to repeat these ν_d calculations for [235]U, [238]U, and [239]Pu. The ν_d values increase by 3.58, 0.36, and 0.83%, respectively. For the delayed presursor chains, at least, either the parameters used in the charge dispersion model or the basic model requires refinement and improvement for ENDF/B-V, and the existence of significant even-odd Z dependence above thermal energies appears unlikely.

TABLE X

TOTAL MEV/FISSION FOLLOWING A U235 AND PU239
FISSION BURST

(FAST FISSION, 1- 2 MEV)

TIME SEC	PU239		U235	
	BETA	GAMMA	BETA	GAMMA
1	.198	.150	.306	.225
2	.147	.111	.219	.160
5	8.540-2	6.450-2	.121	8.825-2
10	5.110-2	3.988-2	6.945-2	5.295-2
20	2.799-2	2.358-2	3.564-2	3.042-2
30	1.913-2	1.686-2	2.315-2	2.132-2
50	1.175-2	1.068-2	1.339-2	1.325-2
80	7.375-3	6.715-3	8.030-3	8.235-3
100	5.820-3	5.290-3	6.245-3	6.450-3
200	2.607-3	2.273-3	2.752-3	2.809-3
300	1.603-3	1.384-3	1.692-3	1.699-3
500	9.070-4	8.050-4	9.400-4	9.500-4
800	5.585-4	5.430-4	5.655-4	6.035-4
1000	4.429-4	4.560-4	4.473-4	4.971-4
2000	2.006-4	2.536-4	2.082-4	2.738-4
3000	1.157-4	1.674-4	1.243-4	1.827-4
5000	5.430-5	8.900-5	6.165-5	1.007-4
8000	2.701-5	4.556-5	3.292-5	5.370-5
10000	1.977-5	3.260-5	2.485-5	3.861-5
20000	8.225-6	1.003-5	1.095-5	1.229-5
50000	2.811-6	2.991-6	3.567-6	3.245-6
100000	1.068-6	1.330-6	1.207-6	1.349-6
200000	3.797-7	5.790-7	3.874-7	5.565-7
700000	7.625-8	1.580-7	7.860-8	1.507-7

TABLE XI

TOTAL MEV/FISS FROM NON-GASEOUS FISSION PRODUCTS

TIME SEC	PU239		U235	
	BETA	GAMMA	BETA	GAMMA
1	0.181	0.132	0.260	0.187
2	0.133	9.708-2	0.183	0.130
5	7.617-2	5.571-2	9.870-2	6.993-2
10	4.482-2	3.402-2	5.532-2	4.108-2
20	2.385-2	1.975-2	2.721-2	2.300-2
30	1.600-2	1.400-2	1.723-2	1.592-2
50	9.661-3	8.818-3	9.797-3	9.840-3
80	6.027-3	5.565-3	5.883-3	6.178-3
100	4.758-3	4.408-3	4.598-3	4.885-3
200	2.160-3	1.939-3	2.094-3	2.222-3
300	1.346-3	1.203-3	1.323-3	1.382-3
500	7.826-4	7.120-4	7.676-4	7.979-4
800	5.007-4	4.837-4	4.875-4	5.187-4
1000	4.040-4	4.057-4	3.951-4	4.296-4
2000	1.863-4	2.193-4	1.885-4	2.315-4
3000	1.054-4	1.391-4	1.101-4	1.478-4
5000	4.714-5	6.710-5	5.189-5	7.347-5
8000	2.215-5	3.004-5	2.641-5	3.412-5
10000	1.595-5	2.036-5	1.980-5	2.328-5
20000	6.795-6	5.773-6	9.254-6	7.006-6
50000	2.191-6	1.565-6	2.977-6	1.816-6
100000	7.488-7	6.792-7	9.122-7	7.486-7
200000	2.632-7	2.943-7	2.799-7	2.976-7
700000	5.540-8	9.264-8	5.997-8	9.262-8

TABLE XII

ENDF/B-IV CALCULATED AND EVALUATED
PROMPT AND DELAYED NEUTRON COMPARISONS

Fission	Delayed Neutrons/100 Fissions		Prompt Neutrons per Fission	
Nuclide	Calculated[a]	Evaluated[b]	Calculated[a]	Evaluated[c]
235U(T)	1.604	1.67±0.07	2.41	2.40
235U(F)	1.483	1.67±0.07	2.38	2.53-2.65
235U(HE)	1.095	0.90±0.1	3.63	4.38-4.51
238U(F)	2.934	4.60±0.25	2.70	2.43-2.58
238U(HE)	1.963	2.6 ±0.2	4.02	4.43-4.58
239PU(T)	0.520	0.645±0.04	2.92	2.87
239PU(F)	0.508	0.645±0.04	2.77	3.01-3.15
241PU(T)	1.047	1.57±0.15	3.00	2.92
233U(T)	0.821	0.740±.04	2.47	--
232Th(F)	3.933	5.27±0.4	2.39	--

[a]These calculations were made using branching probabilities from the FP file and fission yield values given with the fissionable nuclide.

[b]ENDF/B-IV evaluation discussed in "Delayed Neutron Data -- Review and Evaluation," S. A. Cox, ANL/NDM-5, April 1974 (uncertainties are also taken from this report).

[c]Thermal (T) values are at 0.0253 eV. Fast (F) are given at 1.0 and 2.0 MeV. High Energy (HE) are given at 14 and 15 MeV (linear-linear interpolation applies).

TABLE XIII

DELAYED NEUTRONS PER 100 FISSIONS PU239F

GROUP	NUCLIDE	D.N.Y. PER 100 FISSIONS	PERCENT OF TOTAL
2	53I 137	.1247	24.54
4	37RB 94	.0579	11.39
4	39Y 97	.0535	10.53
5	39Y 99	.0372	7.32
4	53I 139	.0321	6.32
3	53I 138	.0245	4.82
2	35BR 88	.0201	3.96
5	53I 140	.0201	3.96
3	37RB 93	.0186	3.66
3	35BR 89	.0171	3.36
1	35BR 87	.0132	2.60
5	37RB 95	.0122	2.40
6	39Y 98	.0099	1.95
4	55CS143	.0088	1.73
4	35BR 90	.0078	1.53
4	51SB135	.0058	1.14
4	33AS 85	.0051	1.00
2	52TE136	.0047	.925
6	37RB 96	.0047	.925
4	55CS142	.0040	.787
2	55CS141	.0028	.551
5	49IN130	.0025	.492
4	36KR 93	.0024	.472
4	55CS144	.0022	.433
5	49IN129	.0016	.315
5	55CS145	.0016	.315
6	49IN131	.0013	.256
6	37RB 97	.0011	.216
3	52TE137	.0010	.197
5	53I 141	.0010	.197
5	35BR 91	.0009	.177
5	38SR 98	.0009	.177
4	54XE142	.0009	.177
3	49IN128	.0008	.157
6	38SR 97	.0006	.118
4	54XE141	.0005	.098
6	35BR 92	.0005	.098
6	36KR 94	.0005	.098
4	49IN127	.0004	.079
5	33AS 86	.0003	.059
6	54XE143	.0003	.059
2	51SB134	.0002	.039
3	34SE 87	.0002	.039
3	37RB 92	.0002	.039
4	32GE 84	.0002	.039
4	34SE 88	.0002	.039
5	34SE 89	.0002	.039
6	33AS 87	.0002	.039
6	55CS146	.0002	.039
3	33AS 84	.0001	.020
4	36KR 92	.0001	.020
6	37RB 98	.0001	.020
4	31GA 80	.00002	.0039
4	32GE 83	.00002	.0039
4	31GA 79	.00001	.002
4	50SN133	.00001	.002
6	37RB 99	.00001	.002

TABLE XIV

DELAYED NEUTRONS PER 100 FISSIONS PU239T

GROUP	NUCLIDE	D.N.Y. PER 100 FISSIONS	PERCENT OF TOTAL
2	53I 137	.1142	21.96
4	37RB 94	.0682	13.11
4	39Y 97	.0591	11.36
5	39Y 99	.0387	7.44
4	53I 139	.0323	6.21
2	35BR 88	.0285	5.48
3	53I 138	.0206	3.96
3	37RB 93	.0199	3.83
3	35BR 89	.0194	3.73
1	35BR 87	.0178	3.42
5	53I 140	.0159	3.06
3	37RB 95	.0126	2.42
3	39Y 98	.0110	2.12
4	35BR 90	.0091	1.75
4	55CS143	.0068	1.31
6	37RB 96	.0061	1.17
4	33AS 85	.0042	.808
2	52TE136	.0038	.731
4	51SB135	.0033	.635
4	55CS142	.0033	.635
4	36KR 93	.0026	.500
2	55CS141	.0024	.461
5	49IN130	.0022	.423
4	55CS144	.0018	.346
5	49IN129	.0017	.327
5	55CS145	.0017	.327
6	37RB 97	.0015	.288
3	35BR 91	.0011	.212
5	38SR 98	.0011	.212
6	49IN131	.0010	.192
3	49IN128	.0009	.173
6	38SR 97	.0008	.154
3	52TE137	.0008	.154
6	33AS 87	.0007	.135
6	36KR 94	.0007	.135
6	35BR 92	.0006	.115
3	34SE 87	.0005	.096
5	53I 141	.0005	.096
4	49IN127	.0004	.077
4	54XE142	.0004	.077
5	34SE 89	.0003	.058
5	33AS 86	.0002	.038
4	34SE 88	.0002	.038
3	37RB 92	.0002	.038
6	37RB 98	.0002	.038
4	54XE141	.0002	.038
4	32GE 84	.0001	.019
4	36KR 92	.0001	.019
2	51SB134	.0001	.019
6	54XE143	.0001	.019
6	55CS146	.0001	.019
3	33AS 84	.00008	.014
4	31GA 80	.00003	.006
4	31GA 79	.00001	.002
4	32GE 83	.00001	.002
6	37RB 99	.00001	.002
4	50SN133	.00001	.002

TABLE XV

DELAYED NEUTRONS PER 100 FISSIONS U235T

GROUP	NUCLIDE	D.N.Y. PER 100 FISSIONS	PERCENT OF TOTAL
4	37RB 94	.1920	11.97
2	53I 137	.1762	10.98
3	35BR 89	.1673	10.43
4	35BR 90	.1616	10.07
2	35BR 88	.1160	7.23
4	39Y 97	.0809	5.04
5	39Y 99	.0765	4.77
4	53I 139	.0756	4.71
5	53I 140	.0724	4.51
5	37RB 95	.0644	4.01
3	37RB 93	.0583	3.63
1	35BR 87	.0505	3.13
3	53I 137	.0411	2.56
4	33AS 85	.0409	2.55
5	35BR 91	.0298	1.86
6	37RB 96	.0245	1.53
6	33AS 87	.0218	1.36
4	55CS143	.0175	1.09
6	39Y 98	.0173	1.08
4	36KR 93	.0171	1.07
4	51SB135	.0159	.991
6	36KR 94	.0104	.648
2	52TE136	.0095	.592
6	37RB 97	.0072	.449
4	55CS142	.0059	.368
6	35BR 92	.0047	.293
5	33AS 86	.0044	.274
5	34SE 89	.0044	.274
5	53I 141	.0040	.249
5	38SR 98	.0035	.218
2	55CS141	.0032	.199
4	55CS144	.0032	.199
5	49IN130	.0031	.193
5	55CS145	.0030	.187
6	49IN131	.0021	.131
3	52TE137	.0021	.131
4	54XE142	.0019	.118
3	34SE 87	.0018	.112
6	38SR 97	.0018	.112
4	34SE 88	.0017	.106
4	32GE 84	.0015	.093
6	37RB 98	.0013	.081
5	49IN129	.0013	.081
3	49IN128	.0007	.044
4	54XE141	.0007	.044
4	36KR 92	.0006	.037
3	37BR 92	.0006	.037
6	54XE143	.0006	.037
3	33AS 84	.0004	.025
6	55CS146	.0003	.019
4	31GA 80	.0002	.012
4	32GE 83	.0002	.012
6	37RB 99	.0002	.012
4	49IN127	.0002	.012
2	51SB134	.0002	.012
4	50SN133	.00004	.002
4	31GA 79	.00002	.001

TABLE XVI

DELAYED NEUTRONS PER 100 FISSIONS U238F

GROUP	NUCLIDE	D.N.Y. PER 100 FISSIONS	PERCENT OF TOTAL
5	53I 140	.3672	12.52
2	53I 137	.3061	10.43
4	53I 139	.2659	9.06
4	37RB 94	.2633	8.98
5	39Y 99	.1677	5.72
3	35BR 89	.1504	5.13
4	35BR 90	.1277	4.35
3	53I 138	.1094	3.73
5	37RB 95	.1068	3.64
6	37RB 96	.1035	3.53
4	51SB135	.1009	3.44
2	35BR 88	.0909	3.10
4	39Y 97	.0861	2.93
3	37RB 93	.0647	2.21
4	33AS 85	.0532	1.81
4	36KR 93	.0486	1.66
6	35BR 92	.0460	1.57
1	35BR 87	.0340	1.16
5	35BR 91	.0337	1.15
5	53I 141	.0334	1.14
4	55CS143	.0303	1.03
6	49IN131	.0302	1.03
5	55CS145	.0256	.873
6	39Y 98	.0241	.822
5	49IN130	.0225	.767
2	52TE136	.0216	.736
6	36KR 94	.0210	.716
6	33AS 87	.0205	.700
4	55CS144	.0194	.661
6	37RB 98	.0186	.634
6	37RB 97	.0163	.556
5	34SE 89	.0155	.528
3	52TE137	.0140	.477
5	38SR 98	.0118	.402
4	54XE142	.0109	.372
4	32GE 84	.0106	.361
5	49IN129	.0100	.341
4	55CS142	.0091	.310
5	33AS 86	.0066	.225
6	54XE143	.0052	.177
6	55CS146	.0049	.167
4	34SE 88	.0040	.136
2	55CS141	.0037	.126
3	49IN128	.0033	.112
6	38SR 97	.0031	.106
6	37RB 99	.0030	.102
3	34SE 87	.0018	.061
4	54XE141	.0017	.058
2	51SB134	.0014	.048
4	36KR 92	.0011	.037
3	33AS 84	.0007	.024
3	37RB 92	.0005	.017
4	49IN127	.0005	.017
4	50SN133	.0003	.010
4	31GA 80	.0002	.007
4	32GE 83	.0002	.007
4	31GA 79	.00002	.0007

TABLE XVII

DELAYED NEUTRONS PER 100 FISSIONS U235F

GROUP	NUCLIDE	D.N.Y. PER 100 FISSIONS	PERCENT OF TOTAL
4	37RB 94	.2387	16.10
2	53I 137	.1780	12.01
3	35BR 89	.1364	9.20
2	35BR 88	.1065	7.18
4	35BR 90	.0920	6.21
4	39Y 97	.0820	5.53
5	39Y 99	.0762	5.14
5	37RB 95	.0645	4.35
4	53I 139	.0593	4.00
3	37RB 93	.0497	3.35
1	35BR 87	.0492	3.32
5	53I 140	.0466	3.14
4	33AS 85	.0457	3.08
3	53I 138	.0445	3.00
6	37RB 96	.0335	2.26
6	39Y 98	.0182	1.23
4	51SB135	.0151	1.02
4	55CS143	.0151	1.02
5	35BR 91	.0128	.863
6	37RB 97	.0106	.715
4	36KR 93	.0093	.627
2	52TE136	.0087	.587
6	33AS 87	.0077	.519
6	36KR 94	.0074	.499
6	35BR 92	.0066	.445
5	34SE 89	.0062	.418
4	55CS142	.0062	.418
4	55CS144	.0059	.398
5	49IN130	.0049	.330
5	55CS145	.0044	.297
4	32GE 84	.0039	.263
5	33AS 86	.0039	.263
5	38SR 98	.0039	.263
6	49IN131	.0036	.243
2	55CS141	.0033	.223
3	52TE137	.0026	.175
4	34SE 88	.0024	.162
4	54XE142	.0023	.155
6	38SR 97	.0020	.135
5	53I 141	.0019	.128
5	49IN129	.0018	.121
3	34SE 87	.0017	.115
6	37RB 98	.0016	.108
3	49IN128	.0013	.088
6	54XE143	.0007	.047
3	33AS 84	.0005	.034
3	37RB 92	.0005	.034
4	54XE141	.0005	.034
6	55CS146	.0005	.034
4	36KR 92	.0004	.027
4	49IN127	.0004	.027
2	51SB134	.0004	.027
4	31GA 80	.0002	.013
4	32GE 83	.0002	.013
6	37RB 99	.0001	.007
4	31GA 79	.00004	.003
4	50SN133	.00004	.003

G. Fission-Product Gamma-Ray and Photoneutron Spectra (M. G. Stamatelatos, T. R. England, and N. L. Whittemore)

Fission-product gamma-ray and photoneutron spectra from thermal- and/or fast-, and/or 14-MeV-neutron fission of ^{232}Th, ^{233}U, ^{235}U, ^{238}U, ^{239}Pu, and ^{241}Pu have been calculated at 27 time intervals between 1 and 1000 h, following reactor shutdown and a nominal constant irradiation period of 1 month.

The gamma spectral calculations were made with a recent version of the CINDER code[46] using ENDF/B-IV yield and decay data for all fission products with half-lives $\geq$ 15 min and gamma energies above the ^{9}Be$(\gamma,n)^8$Be threshold.

The photoneutron spectra were calculated with PHONEX[32] for the two most important photoneutron contributors in fission reactors, ^{9}Be and ^{2}H.

Time-dependent distributions of photons and photoneutrons/fission were calculated, and fitting to simple functions is in progress. For example, it was found that for ^{235}U fission, the normalized time-dependent fission-product gamma-ray intensity per watt of operating power between 3 and 700 h following reactor shutdown could be fitted to within 1% with the following sum of exponentials:

$$I_\gamma = \sum_{i=1}^{3} A_i e^{-\lambda_i t} \quad (E_\gamma > 2.2246 \text{ MeV}) \qquad (3)$$

where $A_1 = 0.9800$, $A_2 = 0.0488$, $A_3 = 0.00612$

$\lambda_1 = 0.3156$, $\lambda_2 = 0.00254$, $\lambda_3 = 0.00093$.

For further details on the spectral results, see Ref. 47, presented at the Conference on Nuclear Cross Sections and Technology, Washington, D. C., March 1975.

VII. MEDIUM ENERGY LIBRARY (D. G. Foster, Jr., W. B. Wilson, and D. R. Harris)

Extensive tests on the Monte Carlo histories of 38 500 800-MeV protons interacting with ^{16}O have shown that it requires about 300 Legendre coefficients to represent the angular distributions of secondary nucleons to an accuracy significantly better than the statistics of the Monte Carlo calculation. Accordingly, we have abandoned the use of such expansions to generate the equal-probability

boundaries for the NASA working library. A new version of NASPRO is nearly completed, which begins by binning the histories in 140 cosine bins, and determines the 11 equal-probability cosine boundaries by linear interpretation. Even with 140 fine groups, this method takes less computation time than the Legendre expansion, and the accuracy is substantially better than the statistics . The cosine bin structure is a subdivision of the equal-probability mesh determined by a previous run, either at a nearby primary energy or on a small portion of the set which is being processed.

REFERENCES

1. N. Jarmie et al., "Elastic Scattering of 7-12 MeV Tritons by Alpha Particles," Bull. Am. Phys. Soc. 20, 596 (1975).

2. M. Karim and J. C. Overley, "Analyzing Powers of the ^{6}Li(n,t) Reaction," Bull. Am. Phys. Soc. 20, 167 (1975).

3. A. Gilbert and A. G. W. Cameron, "A Composite Nuclear Level Density Formula with Shell Corrections," Can. J. Phys. 43, 1446 (1965).

4. P. G. Young, "Nuclear Models and Data for Gamma-Ray Production," Proc. of Conf. on Nuclear Cross Sections and Technology, Wash. D. C. (1975), to be published.

5. D. M. Drake, E. D. Arthur, and M. G. Silbert, "Fourteen-MeV, Neutron-Induced Gamma-Ray Production Cross Sections," Los Alamos Scientific Laboratory report LA-5662-MS (1974); E. D. Arthur, D. M. Drake, M. G. Silbert, and P. G. Young, "Fourteen-MeV, Neutron-Induced Gamma-Ray Production Cross Sections for Several Elements," Bull. Am. Phys. Soc. 20, 166 (1975).

6. D. Wilmore and P. C. Hodgson, "The Calculation of Neutron Cross-Sections from Optical Potentials," Nucl. Phys. 55, 673 (1964).

7. S. A. Caspersson et al., "Economic and Nuclear Performance Characteristics of 500-Mw(e) Oxide, Carbide, and Nitride LMFBR's," presented at ANS Atlanta Section Topical Meeting, Advanced Reactors: Physics, Design, and Economics (Atlanta, Georgia, September 1974).

8. B. Zeitnitz et al., "Neutron Scattering from ^{15}N," Nucl. Phys. A166, 443 (1971).

9. V. V. Verbinski and R. E. Sund, "Measurement of Prompt Gamma Rays from Thermal-Neutron Fission of ^{235}U and ^{239}Pu and from Spontaneous Fission of ^{252}Cf," General Atomic report GA-9148 (1969).

10. R. E. Sund, H. Weber, and V. V. Verbinski, "Isomeric Gamma Rays from ^{235}U(n,f) and ^{239}Pu(n,f) for Times Less than 1 NSec After Fission," Phys. Rev. C10, 853 (1974).

11. R. E. Sund and R. B. Walton, "Gamma Rays from Short-Lived Fission-Fragment Isomers," Phys. Rev. 146, 824 (1966).

12. R. B. Walton and R. E. Sund, "Delayed γ-Rays between 2 and 80 μsec after ^{235}U(n,f) and ^{239}Pu(n,f)," Phys. Rev. 178, 1894 (1969).

13. P. C. Fisher and L. B. Engle, "Delayed Gamma Rays from Fast-Neutron Fission of ^{232}Th, ^{233}U, ^{235}U, ^{238}U, and ^{239}Pu," Phys. Rev. 134, B796 (1964).

14. B. M. Carmichael, "Standard Interface Files and Procedures for Reactor Physics Codes, Version III," Los Alamos Scientific Laboratory report LA-5486-MS (1974).

15. G. M. Hale, D. R. Harris, and R. E. MacFarlane, Eds., "Applied Nuclear Data Research and Development Quarterly Progress Report, April 1 through June 30, 1974." Los Alamos Scientific Laboratory report LA-5727-PR (1974).

16. R. W. Hardie and W. W. Little, Jr., "1DX, A One-Dimensional Diffusion Code for Generating Effective Nuclear Cross Sections," Battelle Northwest Laboratory report BNWL-954 (1959).

17. C. E. Till, L. G. LeSage, R. A. Karam, et al., "ZPR-6 Assemblies 6A and 7; Benchmark Specifications for the Two Large Single-Core-Zone Critical Assemblies -- ^{235}U-Fueled Assembly 6A and Plutonium-Fueled Assembly 7 -- LMFBR Demonstartion Reactor Benchmark Program," Argonne National Laboratory Applied Physics Division Annual Report, July 1, 1970 to June 30, 1971, pp. 86-101, ANL-7910; also ZPR-TM-75.

18. I. I. Bondarenko, Ed., Group Constants for Nuclear Reactor Calculations, Consultants Bureau, New York (1964).

19. R. B. Kidman, R. E. Schenter, R. W. Hardie, and W. W. Little, "The Shielding Factor Method of Generating Multigroup Cross Sections for Fast Reactor Analysis," Nucl. Sci. Eng. 48, 189 (1972).

20. R. E. Schenter, J. L. Baker, and R. B. Kidman, "ETOX, A Code to Calculate Group Constants for Nuclear Reactor Calculations," Battelle Northwest Laboratory report BNWL-1002 (1969).

21. B. A. Hutchins and L. N. Price, "ENDRUN-1, A Computer Code to Generate a Generalized Multigroup Data File from ENDF/B," General Electric Co. report GEAP-13592 (1970).

22. C. L. Cowan, B. A. Hutchins, and J. E. Turner, "TDOWN-1, A Code to Compute Composition-Dependent Cross-Sections," General Electric Co. report GEAP-13740 (1971).

23. W. M. Stacey, Jr., "The Effect of Wide Scattering Resonances on Neutron Multigroup Cross Sections," Nucl. Sci. Eng. 29 (1972).

24. C. R. Weisbin and R. J. LaBauve, "Specification of a Generally Useful Multigroup Structure for Neutron Transport," Los Alamos Scientific Laboratory report LA-5277-MS (1973).

25. O. Ozer, Ed., "Description of the ENDF/B Processing Codes and Retrieval Subroutines," Brookhaven National Laboratory report BNL-50300 (ENDF 11) (June 1971).

26. R. J. LaBauve, C. R. Weisbin, R. E. Seamon, M. E. Battat, D. R. Harris, P. G. Young, and M. M. Klein, "PENDF: A Library of Nuclear Data for Monte Carlo Calculations Derived from Data in ENDF/B Format," Los Alamos Scientific Laboratory report LA-5687 (1974).

27. D. E. Cullen, "Program SIGMA1 (Version 74-1)," Lawrence Livermore Laboratory report UCID-16426 (January 1974).

28. D. J. Dudziak, R. E. Seamon, and D. V. Susco, "LAPHANO: A P_0 Multigroup Photon-Production Matrix and Source Code for ENDF," Los Alamos Scientific Laboratory report LA-4750-MS (ENDF-156) (1967).

29. B. J. Toppel, A. L. Rago, and D. M. O'Shea, "MC^2, A Code to Calculate Multigroup Cross Sections," Argonne National Laboratory report ANL-7318 (1967).

30. W. W. Clendenin, "Calculation of Thermal Neutron Diffusion Length and Group Cross Sections: The GLEN Program," Los Alamos Scientific Laboratory report LA-3893 (1968).

31. C. R. Weisbin, P. D. Soran, D. R. Harris, R. J. LaBauve, and J. S. Hendricks, "MINX, A Multigroup Interpretation of Nuclear X-Sections," Trans. Am. Nucl. Soc. 16, 127 (1973).

32. M. G. Stamatelatos, "PHONEX, A Computer Program to Calculate Photoneutron Spectra," Los Alamos Scientific Laboratory report LA-5860-MS (1975).

33. D. W. Muir and M. E. Wyman, "Neutronic Analysis of a Tritium-Production Integral Experiment," Proc. of the Conf. on the Technology of Controlled Thermonuclear Fusion Experiments, Austin, p. 910 (1972).

34. M. E. Wyman, "An Integral Experiment to Measure the Tritium Production from ^{7}Li by 14-MeV Neutrons in a Lithium Deuteride Sphere," Los Alamos Scientific Laboratory report LA-2234 (Rev) (1972).

35. C. E. Lee, "The LS_n Operator Method in Transport Theory," Trans. Am. Nucl. Soc. 18, 149 (1974).

36. K. D. Lathrop, "DTF-IV, A FORTRAN-IV Program for Solving the Multigroup Transport Equation with Anisotropic Scattering, Los Alamos Scientific Laboratory report LA-3373 (1965).

37. E. D. Cashwell, J. R. Neergaard, W. M. Taylor, and G. D. Turner, "MCN: A Neutron Monte Carlo Code," Los Alamos Scientific Laboratory report LA-4751 (1972).

38. A. Horsley and L. Stewart, "Evaluated Neutron Cross Sections for Deuterium," Los Alamos Scientific Laboratory report LA-3271 (1968).

39. K. D. Lathrop and F. W. Brinkley, "Theory and Use of the General Geometry TWOTRAN Program," Los Alamos Scientific Laboratory report LA-4432 (1970).

40. L. L. Carter, Los Alamos Scientific Laboratory, personal communication.

41. D. R. Harris, "ANDYMG3, The Basic Program of a Series of Monte Carlo Programs for Time-Dependent Transport of Particles and Photons," Los Alamos Scientific Laboratory report LA-4539 (1970).

42. G. M. Hale, D. R. Harris, and R. E. MacFarlane, "Applied Nuclear Data Research and Development Quarterly Progress Report, October 1 through December 31, 1974," Los Alamos Scientific Laboratory report LA-5944-PR (1975).

43. J. P. Neulders, University of Louvain, private communication.

44. G. M. Hale, D. R. Harris, and R. E. MacFarlane, "Applied Nuclear Data Research and Development Quarterly Progress Report, January 1 through March 31, 1974," Los Alamos Scientific Laboratory report LA-5655-PR (1974).

45. W. J. Maeck, Ed., "Fast Reactor Fission Yields for ^{233}U, ^{235}U, ^{238}U, and ^{239}Pu and Recommendations for the Determination of Burnup on FBR Mixed Oxide Fuels: An Interim Project report," Idaho Chemical Programs report ICP-1050-I (to be published).

46. T. R. England, R. Wilczynski, and N. L. Whittemore, "CINDER-7: An Interim Report for Users," Los Alamos Scientific Laboratory report LA-5885-MS, (1975).

47. M. G. Stamatelatos and T. R. England, "Fission-Product Gamma-Ray and Photoneutron Spectra," Proc. of the Conf. on Nuclear Cross Sections and Technology (Washington, D. C., March 1975) (to be published).